Batteries & Supercaps

Review
doi.org/10.1002/batt.202400477

Chemistry Europe
European Chemical Societies Publishing

www.batteries-supercaps.org

Advanced Electrolyte Systems with Sultones Additives for High-Voltage Lithium Batteries

Haojie Wan[+],[b] Siqi Zhong[+],[b] Yifan Liu[+],[a] Yifei Xiong,[b] Ting He,[b] Rong Zeng,[b] Shuang Cai,*[a] and Jianwen Liu*[b]

The new energy market is growing rapidly, lithium batteries (LBs) as the most important source of energy supply in the energy storage and power market, has higher requirements for fast charge and long life, so it is necessary to improve the cell voltage and energy density of LBs. However, LBs with high voltage and high energy density will face serious challenges of electrolyte decomposition and electrode corrosion in high voltage environment. Herein, this review summarizes the effects of a series of sultones as electrolyte additives in high voltage electrolytes. It is found that DTD, ES, 1,3-PS, PES, PCS, MMDS, BDTD, BDTT, DTDph, ODTO, FPS, VES and other sultones have excellent properties on stabilizing SEI/CEI formation, inhibiting gas production, and good high temperature resistance. The preferential oxidation/reduction of sultones can protect the electrolyte from decomposition, and the uniform and dense SEI/CEI can also promote Li^+ transport, protect the electrode from corrosion, prevent the growth of lithium dendrites, and promote the insertion and removal of Li^+, so as to improve the cycle life of the high-voltage battery. Therefore, sultones are very suitable as high-voltage LBs electrolyte additives to improve the performance of cells. This review can provide theoretical support for the design of high voltage and high energy density LBs electrolyte and selection of additives in the future.

1. Introduction

1.1. High-Voltage Lithium Batteries

Generally, high-voltage lithium batteries (LBs) are distinguished by their upper-limit charging voltage, which varies according to different cathode materials. For example, nickel-rich ternary cathode materials can be classified into high-voltage (4.35/4.4 V) and normal voltage (< 4.2 V) LBs. The normal voltage batteries have a nominal voltage of 3.6 or 3.7 V, with a typical upper-limit charging voltage of 4.2 V. In contrast, high-voltage LBs have nominal voltages of 3.8 and 3.85 V, with corresponding upper-limit charging voltage of 4.35 and 4.4 V.[1] For ternary high-nickel or ultra-high-nickel materials, as well as binary materials, ultra-high voltage can sometimes exceed 4.6 V and even reach above 5.0 V.

The notable advantage of high-voltage LBs lies in their high energy density, which extends the runtime by 15% to 25% compared to conventional batteries. However, under high-voltage conditions, the decomposition of cathode materials and the cathode-anode cross-talk become more severe, affecting the battery's lifespan and safety.[2] Therefore, high-voltage LBs have significantly different requirements for cathode and anode materials, electrolytes, and separators compared to conventional LBs, necessitating improvements and innovations in these areas.

1.2. The Necessity for the Development of High-Voltage Lithium Batteries

With the adjustment of energy structure, electric vehicles have gradually come into people's view, with pure electric vehicles (EVs) and hybrid electric vehicles (HEVs) progressively occupying the market.[3] In recent years, the rapid development of EVs has placed significant demands on the performance of lithium-ion power batteries. The energy density of the battery determines the single-charge driving range and lifespan of the vehicle, while the safety performance determines the vehicle's operational safety. Direct evidence suggests that the development of high-voltage LBs is an important way to increase the energy density of batteries, as shown in Equation 1.[4] Where E is energy density, V represents operating voltage, and q is battery capacity. Therefore, the development of high-voltage lithium power batteries with high-safety has become a crucial issue for the widespread adoption of EVs.

$$\Delta E = \int V \times q\mathrm{d}q \tag{1}$$

Currently, the most frequently used high voltage cathode materials are lithium nickel cobalt manganese oxides (NCMs). Depending on the content of Ni/Co/Mn, NCM cathodes can be divided into two categories: low-nickel content materials such as $LiNi_{1/3}Co_{1/3}Mn_{1/3}O_2$ (NCM111) and $LiNi_{0.5}Co_{0.2}Mn_{0.3}O_2$(NCM523), and high-nickel content materials such as $LiNi_{0.6}Co_{0.2}Mn_{0.2}O_2$ (NCM622) and $LiNi_{0.8}Co_{0.1}Mn_{0.1}O_2$ (NCM811). Another one is the

[a] Y. Liu,[+] S. Cai
Department of Chemical Engineering, Hubei University of Arts and Science, Xiangyang 441053, P. R China
E-mail: shuangcai@hbuas.edu.cn

[b] H. Wan,[+] S. Zhong,[+] Y. Xiong, T. He, R. Zeng, J. Liu
College of Chemistry and Chemical Engineering & College of New Energy and Electrical Engineering, Hubei University, Wuhan 430062, P. R. China
E-mail: jianwen@hubu.edu.cn

[+] Haojie Wan, Siqi Zhong and Yifan Liu contributed to this work equally.

spinel-type transition metal-doped compounds $LiNi_xM_{2-x}O_4$, among which the most typical one is $LiNi_{0.5}Mn_{1.5}O_4$, with an operating voltage of up to 4.7 V and a specific energy density of 686 Wh kg^{-1}. Additionally, lithium-rich manganese-based cathodes such as Li_2MnO_3-$LiMO_2$ (M=Co, Ni, Fe) also exhibit advantages of high voltage, high capacity, and good safety, etc.

1.3. Electrolytes for High-Voltage Lithium Batteries

The main components of electrolyte for high-voltage LBs are displayed as follows. (1) Lithium Salts: The common lithium salts include lithium hexafluorophosphate ($LiPF_6$) and lithium tetrafluoroborate ($LiBF_4$), etc. Lithium salts are often used as a key component in electrolytes to provide ionic conductivity. (2) Organic Solvents: Common organic solvents include carbonates, esters, polyethers, and polymer electrolytes, etc. Organic solvents can effectively dissolve lithium salts, regulate the viscosity and solubility of the electrolyte, and also provide good ion transport properties thereby increasing the energy density and power density of the battery.[5] (3) Additives: to improve the properties and safety of high-voltage electrolyte, some auxiliary components are usually added to improve the performance of electrolyte. These additives can increase the stability of the electrolyte, prevent overpotential mutation, and inhibit side reactions on metal lithium electrodes. Different components and formulations are required for specific applications to adapt to particular battery designs and requirements.

In those existing NCM cathode systems, when the anode capacity reaches 1000 mAh/g, further improvements in the anode material yield minimal enhancements in energy density. In this case, increasing the battery's energy density can only be achieved by raising the cut-off voltage, which leads to the development of high-voltage batteries. However, conventional electrolytes do not perform well under high voltage like short lifespan and poor safety. Therefore, it is necessary to develop specific electrolyte formulations for high-voltage applications. The improvement of cut-off voltage is constrained by the oxidative stability of traditional commercial ethylene carbonate (EC) ester-based electrolytes. EC acts like a double-edged sword, while it forms an excellent solid electrolyte interface (SEI) film on the graphite anode side, it is also the most easily oxidized component in the electrolyte matrix which greatly limits the development of high-voltage LBs.[6] Fortunately, the battery performance can be enhanced at high cut-off voltages by regulating the solvation structures of the electrolyte or adding film-forming electrolyte additives to create superior CEI(cathode electrolyte interphase)/SEI films. These measures help to suppress side reactions of the electrolyte during operation, thereby improving the battery's performance under high cut-off voltages.

1.4. Sultones Additives

Sultones have known as esters that simultaneously possess S=O and S–O functional groups. There are many types of sultones, and to date, various sultones have been added to battery electrolytes as additives. The S=O and S–O bonds contained in sultones can undergo reduction or oxidation at the anode or cathode during battery cycling, forming SEI and CEI layers. Most sultones can alter the solventized structures of lithium ions, generating a dense and smooth interfacial layer. This leads to reduced internal resistance, faster charge transfer rates, and higher capacity retention. In general, sultones moleculars can be categorized as monoester sultones, bis-sultones, side-chain sultones, etc., as displayed in Figure 1.

2. Monoester Sultones

2.1. Ethylene Sulfate (1,3,2-Dioxathiolane-2,2-Dioxide, DTD)

Ethylene sulfate (DTD), is one of the earliest monoester sultones used as an additive in electrolytes of high-voltage batteries. DTD can significantly improve the SEI interface and enhance the stability of anode. Although DTD has the advantages of accelerating ion transport, reducing internal resistance, inhibiting the growth of lithium dendrites, enhancing cycling stability, and improving battery capacity retention rate, DTD is more prone to discoloration and has insufficient safety performance.

Huang et al. found that DTD can act as a bifunctional electrolyte additive to enhance the stability of the anode of lithium battery. The side reactions between lithium metal and the electrolyte can reduce the average coulombic efficiency (CE). DTD can regulate the solventized structures of Li^+, optimize the SEI, and lower the energy barrier for lithium deposition, reducing the formation of dead lithium (Figure 2a). The results indicate that with the introduction of 5.0 wt.% DTD, the average CE of the Li|Cu half-cell increases from 71.0% over 60 cycles to 95.8% over 275 cycles.[7] Hu et al. proposed synergistic action of DTD and lithium bis(fluorosulfonyl)imide (LiFSI) as electrolyte additives for graphite/$LiFePO_4$ cells. DTD can generate sulfur-rich SEI film at higher voltage, beneficial for reducing voltage polarization and side reactions during fast charging. Using DTD + LiFSI additives can result in higher average CE, faster charge transfer, solventization/desolvation processes, significantly reducing anode internal polarization (Figure 2b). Additionally, higher rate discharge performance during charging can be achieved, which also significantly extends battery life.[8] Meng et al. conducted a study to investigate the individual effects of several additives, including DTD, vinylene carbonate (VEC) and fluoroethylene carbonate (FEC). Among these, lithium batteries with DTD as an additive exhibit the highest initial capacity and lowest resistance during cycling. Additionally, they display the lowest swelling rate after a 2-week storage period.[9] An et al. investigated several electrolyte systems with different additives, including DTD, DTD + propylene-1,3-sultone (PES), methylene methanedisulfonate (MMDS) and silicon-containing (trimethylsilyl phosphate (TTSP) and trimethylsilyl borate (TMSB) reagents, and compared their performance. The results show that electrolyte with sulfur-containing additives exhibit advantages in terms of lower SEI impedance.[10]

Review
doi.org/10.1002/batt.202400477
Chemistry Europe
European Chemical Societies Publishing

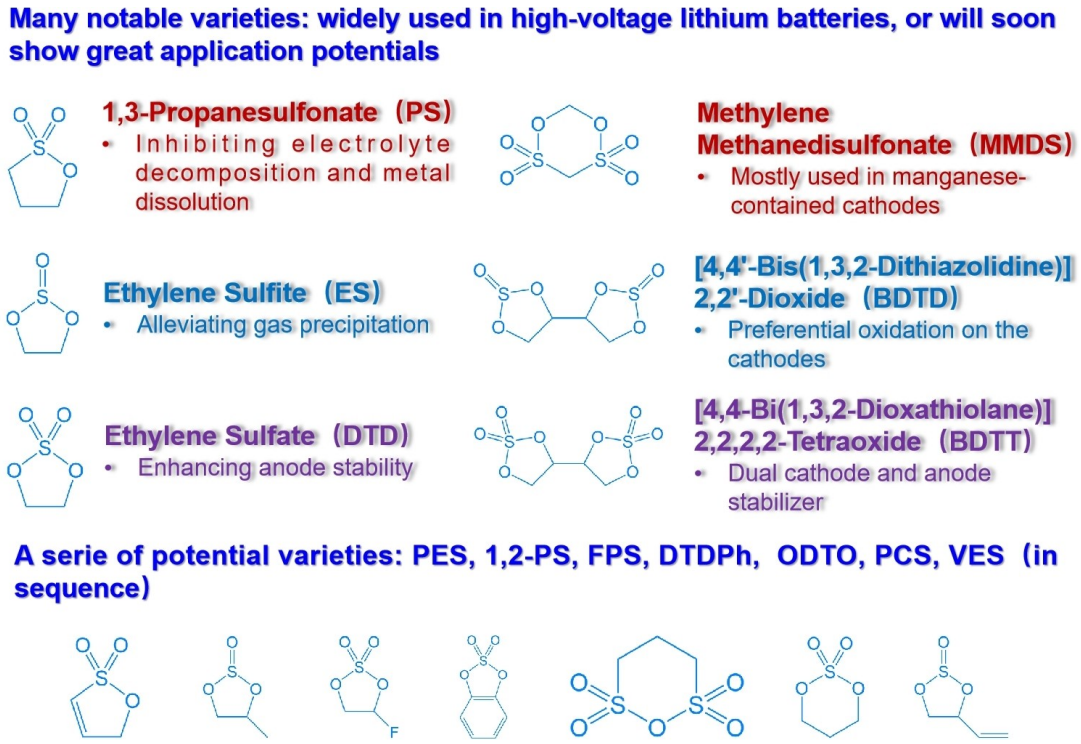

Figure 1. The categorization of sultones moleculars.

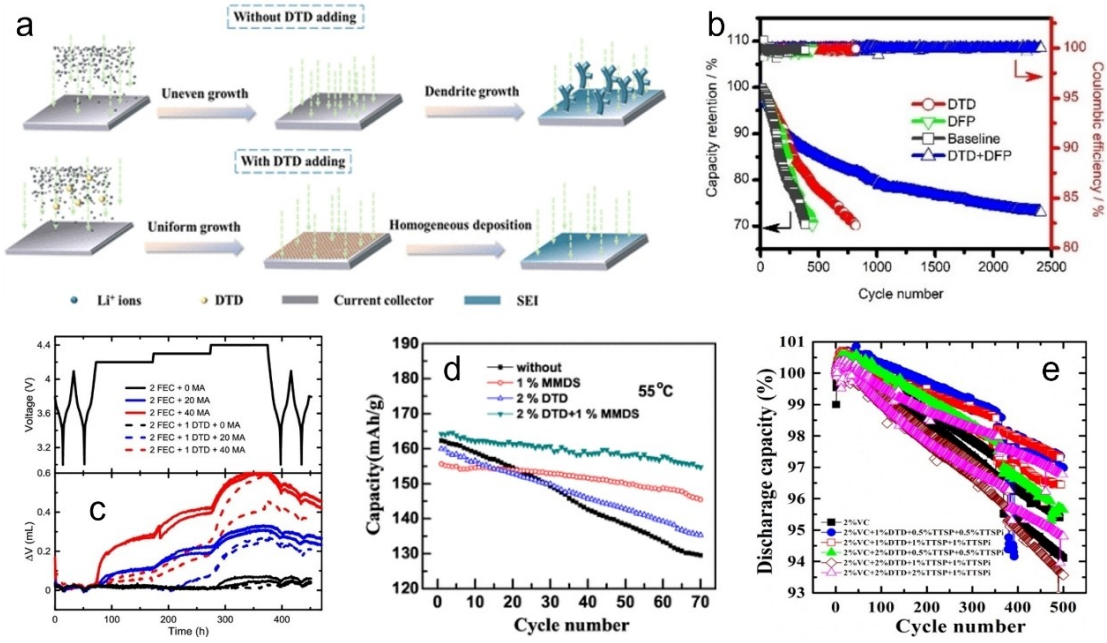

Figure 2. (a) The action of additive DTD on the surface of Li metal. Reproduced with permission.[7] Copyright 2023, the American Chemical Society. (b) Long-term fast-charging cyclability for Gr/LFP pouch cells with Baseline, DTD, DFP and DTD + DFP based electrolytes at 2 C/2 C. Reproduced with permission.[8] Copyright 2022, Wiley. (c) Cell voltage and gas volume during in-situ gas measurements at 40 ± 0.1 °C of EC:DMC (3:7) with 2% FEC and 2% FEC + 1% DTD with 0%, 20%, and 40% MA. Reproduced with permission.[12] Copyright 2018, The Electrochemical Society. (d) Cycle performance of the NCM111 in 1 M $LiPF_6$-EC:EMC electrolyte with different electrolyte under 55 °C. Reproduced with permission.[13] Copyright 2017, Springer Link. (e) Discharge capacity as a function of cycle number for cells containing different additives, tested using currents of C/2.2 at −40 °C. Reproduced with permission.[14] Copyright 2014, The Electrochemical Society.

Taskovic et al. utilized 1.33 M $LiPF_6$ filled $LiNi_{0.5}Mn_{0.3}Co_{0.2}O_2$/graphite cells as the base, employing a ternary electrolyte additive system of ethylene carbonate, ethyl methyl carbonate and dimethyl carbonate (EC:DMC:EMC) in a volume ratio of

25:5:70. They investigated long-term charge-discharge cycling at 20 and 40 °C with different weight percentages of vinylene carbonate (VC) and DTD electrolyte additives. Among these, cells with 1% VC or 2% VC + 1% DTD exhibit the best capacity retention and lowest impedance growth. Most lithium-ion cells containing DTD surpass 1500 cycles under both 20 and 40 °C conditions.[11] Glazier et al. developed a high-rate additive mixture of FEC and DTD for $LiNi_{0.5}Mn_{0.3}Co_{0.2}O_2$/graphite pouch cells. They studied a solvent system composed of EC, EMC and DMC, with additive concentrations of 0%, 20% and 40%. At 4.3 V, the addition of only 1 wt.% DTD added to 2 wt.% FEC improves the properties of cells containing 20% methyl formate (MA) and 40% MA to those of cells without MA and 20% MA, respectively (Figure 2c).[12] Cui et al. studied the use of spherical $LiNi_{1/3}Co_{1/3}Mn_{1/3}O_2$ (NCM111) cathode material with electrolyte additives, either individually or in combination, including DTD and MMDS. The results reveal that DTD additives can enhance the initial CE of NCM111, with spherical NCM111 achieving a maximum initial discharge capacity of 177.81 mAh/g at 2 wt.% DTD and maintaining 92.29% capacity retention after 80 cycles (Figure 2d). The combination of 2 wt.% DTD + 1 wt.% MMDS present the best performance, with capacity retention rates of 102.2% after 80 cycles at room temperature and 94.2% after 70 cycles at 55 °C.[13] David et al. investigated the effects of electrolyte additives, including VC, DTD, trimethylsilyl phosphate (TTSP), and trimethylsilyl phosphite (TTSPi), on $Li[Ni_{1/3}Mn_{1/3}Co_{1/3}]O_2$/graphite pouch cells. Compared to 2% VC alone, the combination of these additives can reduce parasitic reactions on the cathode above 4.1 V, enhance CE, mitigate charge endpoint capacity slippage, and lower battery impedance. The optimal electrolyte formulation is found to be 2% VC + 1% DTD + 0.5% TTSP + 0.5% TTSPi (Figure 2e).[14]

Yu et al. employed a dual-component electrolyte additive of lithium difluorophosphate ($LiPO_2F_2$) and DTD to enhance the stability of interface films. According to theoretical calculations, $LiPO_2F_2$ is more prone to oxidation and decomposition on the cathode surface, whereas DTD exhibits greater propensity for reduction and decomposition on the anode surface compared to other solvents. When applied to NCM523/graphite pouch cells, this novel electrolyte additive effectively improves electrode interface stability and cycling performance (Figure 3a).[15] OuYang et al. studied the safety characteristics of graphite + SiO_x cells and revealed the effects of two additive combinations, 2% VC + 1% DTD, and 2% FEC + 1% lithium difluorophosphate (LFO). Results display that both combinations, 2VC + 1DTD and 2FEC + 1LFO, exhibit flammability and are unable to suppress reactions between the anode material and the electrolyte, thus failing to effectively enhance safety performance (Figure 3b).[16] Ming et al. proposed that SEI forming agents such as EC, sultone, and cyclic sulfate are commonly regarded as film-forming additives in lithium batteries, contributing to enhanced stability of graphite anodes (Figure 3c). The modified Li^+ solventized structures by these additives play a crucial role in facilitating reversible Li^+ insertion into graphite. Adjusting Li^+ coordination structures with DTD helps alleviate graphite exfoliation caused by concurrent Li^+ and solvent co-insertion.[17]

Zhang et al. investigated DTD as an electrolyte additive to enhance lithium storage performance of silicon/graphite composite anodes. Their team analyzed the impact of DTD on the SEI film using scanning electron microscopy (SEM), and identified thin, uniform, and stable SEI film formation through its reduction and decomposition reactions on the electrode surface, confirmed by X-ray photoelectron spectroscopy(XPS) and Fourier transform infrared spectroscopy (FTIR) (Figure 3d). Optimizing the dosage of DTD can improve the lithium storage performance of silicon/graphite anodes.[18] Zheng et al. studied ethyl (2,2,2-trifluoroethyl) carbonate (ETFEC) as a solvent component in high-voltage electrolytes for $LiNi_{0.5}Mn_{1.5}O_4$ (LNMO). When 2% EC or DTD is added to ETFEC, significant improvements in cycling performance are observed, with LNMO

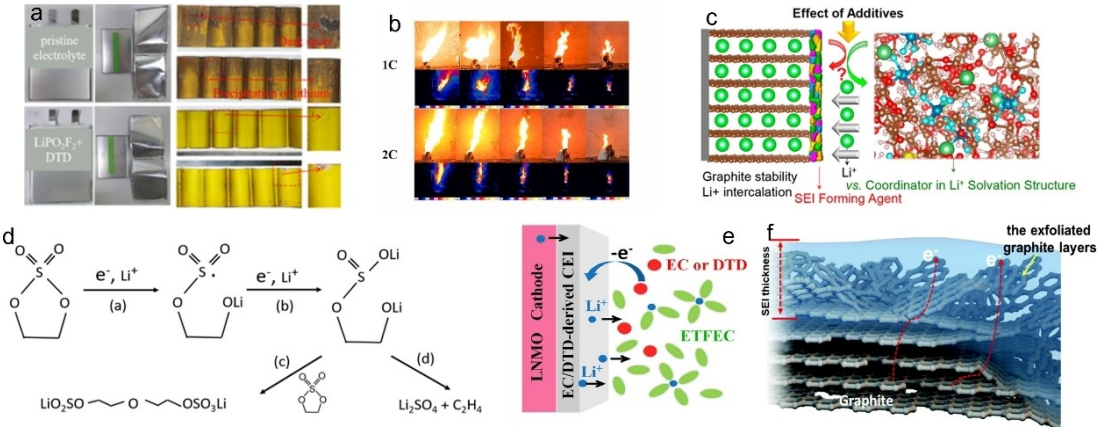

Figure 3. (a) Optical image of NCM 532/C pouch cell with pristine electrolyte and $LiPO_2F_2$ + DTD electrolyte additive after 100 cycles, respectively. Optical image of NCM523 cathode in the pouch cell with pristine electrolyte and $LiPO_2F_2$ + DTD electrolyte additive after disassembling, respectively. Reproduced with permission.[15] Copyright 2022, Springer Link. (b) Typical phenomena of pouch cells overcharged with 1 C and 2 C rates during the overcharge tests. Reproduced with permission.[16] Copyright 2022, Elsevier. (c) Schematic diagram of the components of the SEI after adding DTD. Reproduced with permission.[17] Copyright 2019, The Electrochemical Society. (d) The proposed decomposition mechanism of DTD. Reproduced with permission.[18] Copyright 2020, Word Scientific. (e) The proposed function mechanism of ETFEC and DTD on $LiNi_{0.5}Mn_{1.5}O_4$ batteries. (f) Schematic showing the insertion of $Li(EC)_x$ in the graphite leading to the disruption and exfoliation of near-surface graphite.

maintaining a capacity retention of 93% after 300 cycles. This enhancement can be attributed to the oxidation of additives on the surface of LNMO particles, which contributes to the formation of a cathode/electrolyte interphase film (Figure 3e). This composite CEI film plays a crucial role in suppressing severe electrolyte decomposition under high voltage.[19] Han et al. used cryogenic transmission electron microscopy (cryTEM) to reveal the atomic structure and phase distribution of the SEI. During constant current charging of 0.05 C for 3 hours, propylene carbonate (PC) strips the graphite anode, compromising its structural integrity. At 45 °C and 0.1 C charging for 3 hours, EC/diethyl carbonate (DEC) also cause surface stripping of the graphite anode, embedding detached graphite into the SEI, continuously thickening it (Figure 3f). By comparison, the use of 1 wt.% triphenyl phosphate (TPP), DTD, or FEC additives results in the formation of a stable and thin SEI film.[20]

2.2. Ethylene Sulfite (ES)

Compared to DTD, Ethylene sulfite (ES) lacks one double-bonded oxygen, which displays similar function on batteries, such as building SEI layers, protecting electrodes, and reducing internal resistance, etc. It is also an electrolyte additive suitable for high-voltage and high-rate batteries.

Wang et al. combined ES with lithium difluoroborate (LiDFOB) which has a similar redox potential as a novel electrolyte. Due to synergistic effects, these compounds can simultaneously form an inorganic-organic chain-link protective film on both cathode and anode surfaces. With its simple formulation and high concentration of dilute salt, this electrolyte mitigates issues faced by high-voltage lithium-ion batteries, such as lithium dendrite growth, self-discharge, gas evolution, and dissolution of transition metals (Figure 4a–4c). It achieves 90% capacity retention after 200 cycles at 4.6 V, with an average coulombic efficiency of 99.5%.[21] Zhou et al. investigated capacity anomaly at room temperature of graphite anodes in VC-ES electrolytes under higher rates ($\geq$0.5 C) and provided explanations. Through electrochemical analysis and surface characterization of graphite anodes under various charge-discharge states, they proposed a dynamic evolution mechanism of the SEI. For graphite anodes operating at 55 °C, VC-ES electrolyte outperforms VC electrolyte, demonstrating significant potential for high-temperature batteries (Figure 4d).[22]

Wang et al. studied the influence of additives on the electrochemical performance of PC-based polymers systematically. ES proves to be an effective additive for enhancing capacity retention at high rates, outperforming EC and FEC. The addition of 5 wt.% ES significantly reduces internal resistance, enhances electrochemical stability, and improves low-temperature performance (Figure 4e). This research provides valuable insights into exploring effective electrolyte/additive combinations to reduce internal resistance and enhance low-temperature performance of lithium batteries.[23] Matsuoka et al. discovered that EC and ES as SEI formation additives can suppress the reduction decomposition of acetonitrile (AN) and improve the high-temperature durability of $LiPF_6$ under various cathode chemical compositions. This electrolyte can increase capacity by using thicker electrodes and also reduces the overall cost of battery production (Figure 4f).[24] Suzuki et al. used ES as an electrolyte additive with LiFSA salt, investigating the impact of C_{Li+} variations on the solvation and structure of lithium-ion coordination. When $C_{Li+} < 1$ M, Li^+ fully solvates with ES molecules, forming tetrahedral $[Li(ES)_4]^+$ complexes. As the C_{Li+} increases to 2.5 M, ES interacts with FSA anions to form

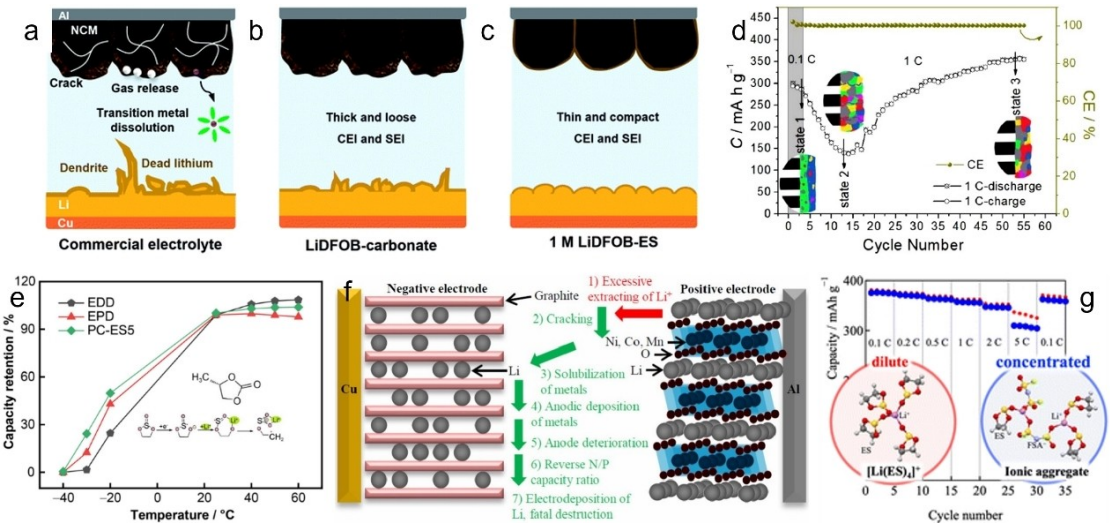

Figure 4. (a–c) The gas release, transition metal dissolution, thick and loose CEI/SEI, thin and compact CEI/SEI based on the commercial or ES-based electrolytes. Reproduced with permission.[21] Copyright 2022, Royal Society of Chemistry. (d) Cycling plot of Gr||LTP/C at 1 C. (e) Low and high-temperature performances of LiC cells with EDD, EPD and PC-ES5 electrolytes with temperature changing from −40 to 60 °C. Reproduced with permission.[23] Copyright 2022, Springer Link. (f) Schematic degradation mechanism of NCM/graphite cells using high ionic conductivity acetonitrile electrolyte. Reproduced with permission.[24] Copyright 2021, Wiley. (g) Discharge capacity of the graphite electrode in 1.0, 3.6, and 4.9 mol dm^{-3} LiFSA/ES solutions at various rates at 298 K. Reproduced with permission.[25] Copyright 2022, Royal Society of Chemistry.

electron-paired bonds. When concentration further increasing to 3 M leads to ion aggregation with multiple lithium-ion complexes connected by several FSA anions (Figure 4g). LiFSA/ES electrolyte solutions exhibit reversible lithium-ion insertion/extraction reactions independent of C_{Li+}, attributed to ES molecules primarily undergoing reduction and forming SEI films. Therefore, even at high lithium concentrations, they demonstrate excellent charge-discharge performance at high rates.[25]

2.3. 1,3-Propane Sultone (1,3-PS)

1,3-propane sultone (1,3-PS), known for significantly enhancing battery performance, has been extensively studied in high-voltage batteries. It preferentially reduces to form the SEI interface layer in electrolytes, inhibits solvent reduction and metal dissolution, reduces gas generation of batteries, improves battery cycling performance and exhibits excellent high-temperature performance.

Xu et al. utilized VC and 1,3-PS to enhance the high-temperature performance of $LiNi_{0.6}Mn_{0.2}Co_{0.2}O_2$/artificial graphite pouch cells. After the addition of these additives, the capacity retention of entire cells reaches 98% after 200 cycles at 45 °C and 500 mA. The results indicate that these additives not only protect the anode but also safeguard the cathode. 1,3-PS can undergo reduction to form sulfides after cycling (Figure 5a). The combination of these two additives optimizes interface reactions, suppresses electrolyte decomposition and manganese dissolution, thereby improving the battery's high-temperature storage performance and cycling stability.[26] Lin et al. investigated the reduction reaction of 1,3-PS on the anode surface of lithium-ion cells to form a SEI film using density functional theory. In the solvent state, the most stable reduction states of PS and EC are identified as initial reactants. With the addition of PS, it preferentially undergoes reduction, thereby inhibiting the reduction of EC and reducing the generation of ethylene gas (Figure 5b). Additionally, compounds formed by PS are lithium-containing compounds with higher reduction capability compared to EC, which is crucial for the formation of an effective SEI film by reducing additives.[27] Oh et al. investigated the high-rate performance of NCM333, NCM622, and NCM811 cathode materials in $LiPF_6$/EC electrolyte with EMC, VC, and PS as additives. Specifically, the addition of VC + PS in the electrolyte suppresses further decomposition of reduction products, thereby providing a stable cathode SEI film during high-rate cycling (Figure 5c). The synergistic effect of VC + PS may stem from the interaction between the ethylene and sultone functionalities. Consequently, particularly for the NCM811 cathode material, the VC + PS additive combination achieved outstanding cycling performance.[28] Yim et al. also investigated the compatibility of VC, succinonitrile (SN), and PS additives with overlithiated layered oxides (OLO) by incorporating them into the electrolyte of electrochemical cells. They found that PS effectively inhibits electrolyte decomposition and metal dissolution, demonstrating excellent capacity retention

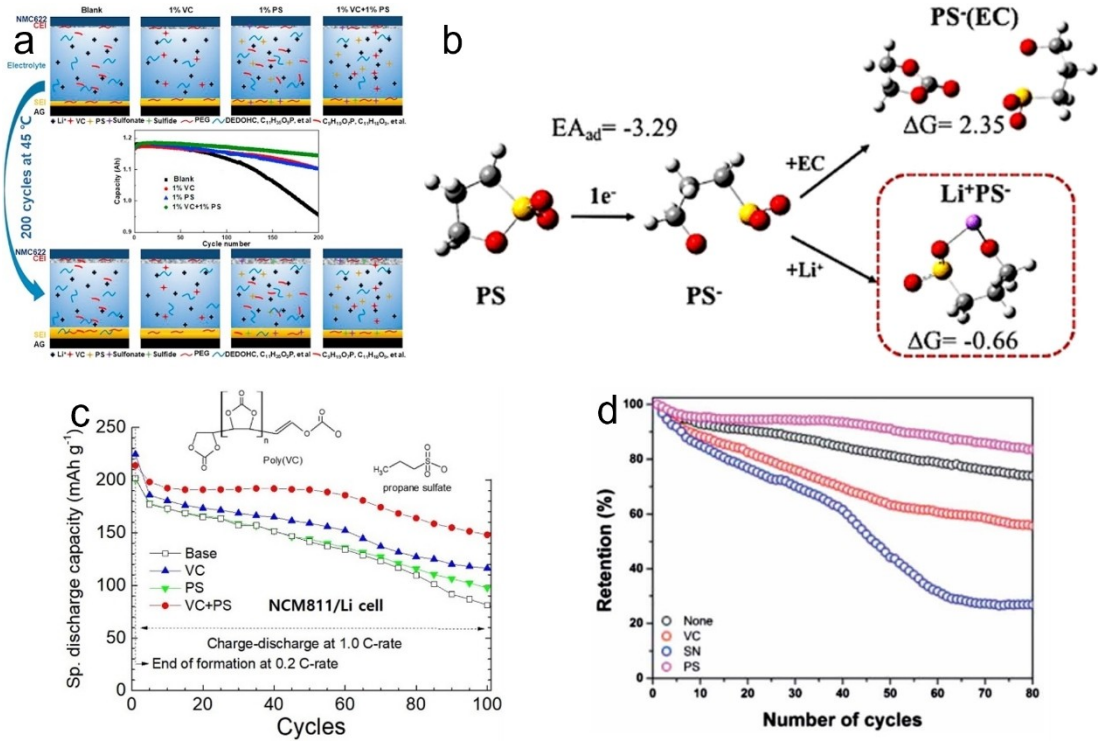

Figure 5. (a) The pouch cells performance with different electrolytes. Cycling performance of the four electrolyte systems at 0.5 C and 45 °C for 200 cycles. Reproduced with permission.[26] Copyright 2019, Elsevier. (b) Optimized structures and charge distributions of EC and PS in different reduction states in the solvent state. (c) Cycling performance of NCM811 materials. Reproduced with permission.[28] Copyright 2020, Elsevier. (d) Full-cell performance of electrolyte with additives. Reproduced with permission.[29] Copyright 2014, Royal Society of Chemistry.

(83.5% remaining discharge capacity after 80 cycles) and low metal dissolution (Figure 5d).[29]

Li et al. studied PS as an electrolyte additive to enhance the cyclability of $LiMn_2O_4$/graphite lithium-ion cells at high temperatures. The charge-discharge testing demonstrates that PS significantly improves the cyclability of $LiMn_2O_4$/graphite pouch cells at 60 °C. Compared to cells without additives, those with 5% PS show an increased capacity retention from 52% to 71% after 180 cycles. The enhancement in cycling performance is attributed to PS modifying the SEI films on both the anode and cathode of the $LiMn_2O_4$/graphite cells, which effectively prevents the structure of anode and cathode from being punctured and inhibited the decomposition of the electrolyte.[30] Xu et al. investigated the impact of the additive PS on the electrolyte/electrode interactions in lithium-ion cells. Using a 1:1:1 EC/DEC/DMC electrolyte blend, lithium-ion cells are cycled and stored for 15 days at 75 °C. The cells with 2% PS show better capacity retention after storage at 75 °C compared to those without PS. After analyzing the electrode surface, the improvement in the performance with PS addition is stemmed from its modification of cathode surface.[31] Hekmatfar et al. studied the impact of three electrolyte additives (VC, PS, and FEC) on the electrochemical performance and CEI properties of NMC532 cells. The addition of VC and PS to the standard electrolyte significantly improves the capacity and cycling stability of the NMC532 electrode in both configurations (Figure 6a). This enhancement is attributed to the formation of a stable and passivating CEI layer.[32] Birrozzi et al. conducted research on the electrolyte additive PS. Results show that PS has positive effects on capacity retention and CE of layered cathodes, thereby improving cycling stability and structural integrity of the cathode. The enhanced capacity retention in batteries with PS is primarily attributed to its involvement in forming a cathode passivation film, which inhibits metal dissolution from the cathode material (Figure 6b).[33]

Pires et al. used PS as a protective additive for lithium-rich cathode materials in [EC-DMC + 1 mol/L $LiPF_6$] electrolyte. The results demonstrate that the addition of 1% PS to the electrolyte can ensure complete activation of the electrodes in the initial cycle and better electrode activation (Figure 6c). As a result, Li//Li-rich-NMC half-cells and Gr//Li-rich-NMC full-cells achieve capacities as high as C = 330 mAh g^{-1} and C = 275 mAh g^{-1} respectively during charge-discharge cycles, with a cutoff voltage of 5 V. Compared to conventional electrolytes, Li//Li-rich-NMC half-cells with PS exhibits higher reversible capacity, superior capacity retention (245 mAh g^{-1} after 240 cycles), excellent CE (99%), and enhanced high-rate discharge capability (over 180 mAh g^{-1} at 1 C discharge rate).[34] Preparation and study of lithium-ion button cells with and without PS and VC in the electrolyte were conducted by Zhang et al. The results indicate that the combination of PS and VC improves capacity retention of lithium-ion button cells during cycling at 55 °C and reduces impedance. The results of ectopic surface analysis confirm that the addition of PS and VC alters the reduction reactions on the anode, thereby inhibiting the formation of ethylene and modifying the structure of the SEI film.[35] Park et al. investigated the role of PS as an additive in lithium battery electrolytes. The addition of PS to PC-based electrolytes significantly suppresses solvent decomposition on graphite electrodes, thereby enhancing the electrochemical performance of the battery (Figure 6d). PS forms a SEI film on the graphite surface before solvent decomposition, which not only inhibits lithium deposition on the graphite electrode surface but also accelerates lithium insertion, resulting in the formation of LiC_6 on the graphite electrode.[36]

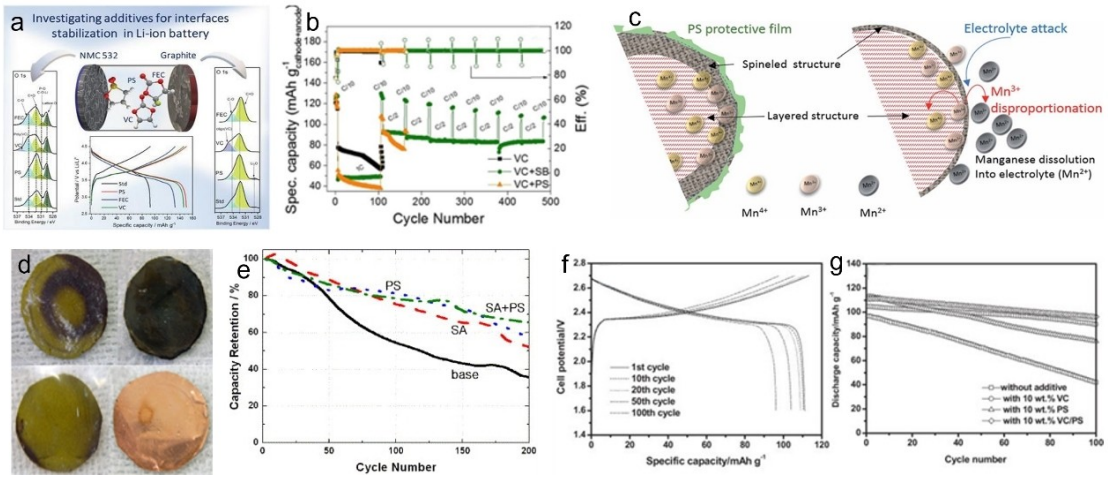

Figure 6. (a) Cycling performance of NMC532//Gr cells employing Std, PS, VC, and FEC in terms of selected potential profiles. (b) Comparison of the longterm cycling performance of cells cycled with pristine, and PS and SB containing electrolytes. Reproduced with permission.[33] Copyright 2016, Elsevier. (c) Schematic of the PS protection mechanism on the Li-rich NMC cathode during cycling and progressive transformation from the layered to the spinel structure. Reproduced with permission.[34] Copyright 2015, Royal Society of Chemistry. (d) Appearance of front side, backside for the natural graphite electrode cycled with or without the electrolyte additive at −5 °C. Reproduced with permission.[36] Copyright 2009, Elsevier. (e) Cycle behavior of LNMO/graphite bicells (50 mA h) at 25 °C with 1 M $LiPF_6$ EC/EMC (1/2, v/v) solutions containing no additive, 2 wt.% SA, 3 wt.% PS, and 2 wt.% SA + 3 wt.% PS. Reproduced with permission.[37] Copyright 2007, Elsevier. (f) Charge and discharge curves of the $Li_4Ti_5O_{12}/LiCoO_2$ cell in ionic liquid electrolyte containing 10 wt.% VC/PS, and (g) discharge capacities as a function of the cycle number for cells with different additives. Reproduced with permission.[38] Copyright 2012, Elsevier.

Lee et al. discovered that SA and PS could significantly extend the cycle life of LNMO/graphite cells and suppress their expansion behavior. The advantages of SA and PS lie not only in their formation of a stable SEI layer on graphite but also in their oxidative stability under high voltage. LNMO/graphite pouch cells using 1 M $LiPF_6$ EC/EMC solution containing SA and PS show approximately 80% capacity retention after 100 cycles (Figure 6e).[37] Kim et al. investigated the cycling behavior of $Li_4Ti_5O_{12}$/$LiCoO_2$ cells in 1-butyl-1-methylpyrrolidinium bis(trifluoromethanesulfonyl)imide (BMP-TFSI) based electrolyte with different additives such as VC, PS and their mixture. Cells assembled with BMP-TFSI containing 10 wt.% VC/PS (weight ratio = 1:1) exhibit high discharge capacity and excellent capacity retention. In the presence of the VC and PS mixture, an electrochemically stable stable SEI is formed on the $Li_4Ti_5O_{12}$ electrode during cycling (Figure 6f and 6 g).[38] Zhou et al. studied the application effects of additives VC, PS, FEC, and DTD in high nickel [$n_{(Ni)} \geq 80\%$] positive electrode materials for lithium batteries. They analyzed the electrochemical performance, gas evolution during formation, and negative electrode interface morphology of Li|SiO_x/graphite pouch cells. The results show that none of the additives except PS affects the initial capacity of SiO_x/ graphite electrodes. VC, PS, and FEC can reduce gas evolution during formation in soft-packed cells.[39]

2.4. Prop-1-Ene-1,3-Sultone (PES)

Prop-1-Ene-1,3-Sultone (PES), which has one more double bond compared to PS, is more easily reduced to form a SEI interface layer. This layer protects the graphite electrode, prevents electrolyte co-intercalation, and suppresses gas evolution, making it an excellent additive for high-voltage and high-temperature electrolytes.

Li et al. proposed PES as an additive in PC-based electrolytes for lithium-ion batteries. Voltammetry results show that PES is more easily reduced than PS. Charge-discharge experiments demonstrate that using PES successfully suppresses co-intercalation of PC with Li^+ in graphite. The performance of $LiCoO_2$/graphite batteries prepared with PES as an additive surpasses those using PS, presenting smaller initial capacity loss and better cycling stability.[40] Ma et al. added 2 wt.% PES + 1 wt.% TTSPi + 1 wt.% MMDS ("PES-211") to EC and EMC (weight ratio = 3:7) electrolyte and cycled pouch cells at different upper cutoff voltages from 4.2 to 4.7 V. The addition of 2% PES or "PES-211" has been proven to suppress the high impedance growth when the cell is cycled to 4.4 V and above. Long-term cycling tests at 3.0 and 4.4 V at 45 °C show that "PES-211" preserves optimal capacity retention (85%) and minimal impedance growth after 500 cycles (Figure 7a). This study indicates that the use of "PES-211" extends the lifespan of NMC/graphite lithium-ion cells, enhances their power output, exhibits better high-voltage tolerance.[41] Li et al. utilized PES as an electrolyte additive to modify the cathode/electrolyte interface. Results demonstrate that the application of PES significantly enhances the cycling stability of the cathode. After 400 cycles at 1 C rate, cells with 1.0 wt.% PES maintain a capacity retention of 90%, whereas cells without additives retain only 49% capacity (Figure 7b and 7c).[42] Li et al. investigated the physicochemical properties of the SEI formed by PES on graphite anodes in PC-based electrolytes for lithium-ion cells. They found that the charge-discharge performance of $LiCoO_2$/

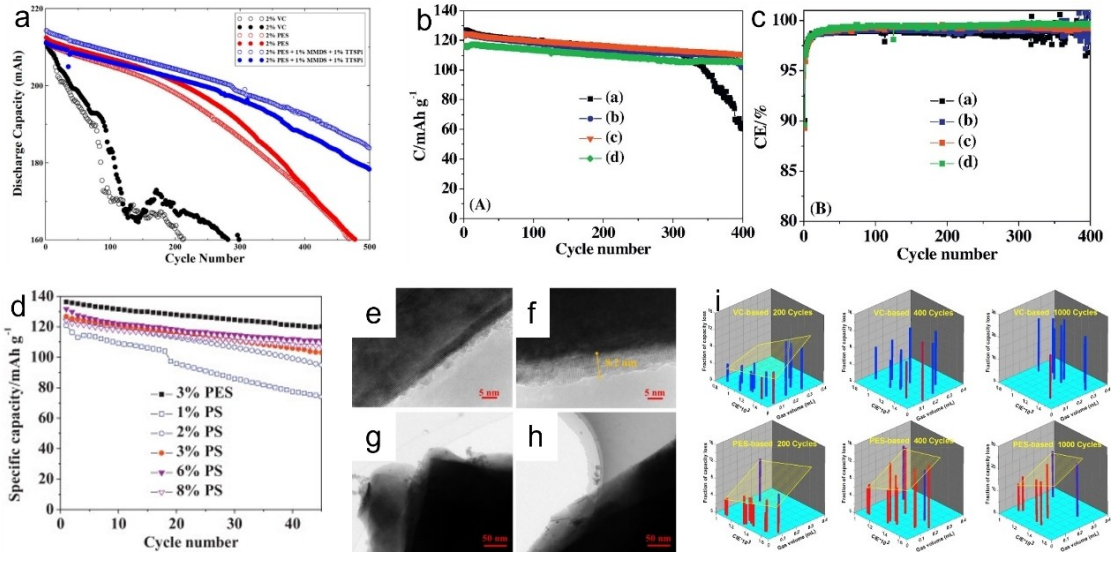

Figure 7. (a) Discharge capacity versus cycle number for NMC442/graphite pouch cells containing the additives 2% VC, 2% PES or "PES-211". Reproduced with permission.[41] Copyright 2014, The Electrochemical Society. (b) Cycling performances of Li/$LiNi_{0.5}Mn_{1.5}O_4$ cells in 1.0 mol dm^{-3} $LiPF_6$/EC-EMC (1:2) electrolyte without, with 0.5 wt.%, 1.0 wt.% and with 2.0 wt.% PES. (c) The charge/discharge cycling performed with 1 C current rate at 25 °C. Reproduced with permission.[42] Copyright 2014, Elsevier. (d) Cycling performances of $LiCoO_2$/graphite cells in 1.0 M $LiPF_6$/PC-EMC (1:1) electrolytes containing various contents of PS, compared with the electrolyte containing 3 wt.% PES. TEM graph of $LiCoO_2$ and graphite particles after 3 cycles in the electrolyte with or without PES. Reproduced with permission.[43] Copyright 2013, Elsevier. (e) $LiCoO_2$ electrode in the electrolyte without PES, (f) $LiCoO_2$ electrode in the electrolyte with 1 wt.% PES, (g) graphite electrodes in the electrolyte without PES, (h) graphite electrode in the electrolyte with 1 wt.% PES. (i) "3-Dimensional" plot of the fraction of capacity lost after 200 cycles, 400 cycles and 1000 cycles as a function of CIE. Reproduced with permission.[45] Copyright 2015, Elsevier.

natural graphite (NG) cells using a PC-based electrolyte containing 3 wt.% PES is superior to those containing 6 wt.% PS. SEM and XPS results indicate that the SEI formed by PES contains more PES reduction products, protecting the graphite structure. (Figure 7d). Meanwhile, sulfur-containing substances are identified as components of the SEI, demonstrating the significant role of PES reduction in SEI formation.[43]

Song et al. studied the effects of PES on graphite anodes and $LiCoO_2$ cathodes systematically. The results indicate that PES can be reduced prior to EC, forming a more stable SEI film on the graphite anode. PES also forms a film on the $LiCoO_2$ electrode, so that $LiCoO_2$/artificial graphite (AG) cells prepared with PES additives exhibit excellent high-temperature performance. Cells with PES can withstand 2 C charge-discharge cycles at 70 °C, maintaining 90.1 % capacity retention after 300 cycles. The SEI film formed by PES inhibits lithium ion insertion/deinsertion and slightly increases cell resistance, but has minimal impact on rate performance and low-temperature performance (Figure 7e–7 h). Thus, even at −40 °C, cells with 1 % PES still maintain a discharge capacity retention rate of 75 %. These results indicate that PES is a promising additive for batteries operating within a wide temperature range.[44] Xia et al. systematically studied the effects of EC-based electrolyte additives and PES additives on high-temperature cycling of graphite pouch cells, investigating capacity decay during cycling, charge transfer resistance before and after cycling, and gas evolution during cycling. Cells with EC-based additives blends exhibit over 20 % initial capacity loss and expanded over 10 % of their initial volume after 1000 cycles at 55 °C (Figure 7i). Cells with PES additives generate significantly less gas than conventional electrolytes. After 1000 cycles, cells with PES additives lose less than 20 % of their initial capacity and exhibit reduced impedance after long-term cycling. Therefore, PES-based electrolytes are more beneficial for graphite cells at high temperatures compared to those EC-based electrolytes.[45]

Xia et al. designed a fluoride-based electrolyte mixture containing 1 M $LiPF_6$/EC:DMC (dimethyl carbonate) (1 : 1) and PES as electrolyte additives, demonstrating excellent cycling and storage performance in $Li(Ni_{0.4}Mn_{0.4}Co_{0.2})O_2$/graphite pouch cells tested at 4.5 V. The study show that adding PES helps control gas evolution in fluoride-based electrolyte cells. Although cells with fluoride-based electrolytes exhibit higher impedance in early cycles, however, these fluorinated electrolytes cells with 1 %, 2 %, and 3 % PES additives, perform better than those non-fluorinated electrolytes cells under all tests during charge/discharge cycling to 4.5 V (Figure 8a–8d).[46] Xia et al. systematically investigated the effects of six additives [VC, ES, DTD, 1,3-propanediol cyclic sulfate (PCS), PS, and PES] on the electrochemical performance of nickel cobalt manganese oxide (NCM111)//graphite lithium-ion cell systems. By comparing initial charge-discharge efficiency, discharge capacity, rate capability, low-temperature discharge capability, high-temperature storage performance, and cycle life, they found that sultone-based additives (PS and PES) excel in suppressing high-temperature gas generation (Figure 8e). Due to the bifunctional group, PES exhibits superior cycling performance and better ability to suppress voltage decay compared to PS.[47] Qiao et al. selected PES and MMDS as electrolyte additives for silicon-carbon negative electrode, focusing on their impact on high-temperature performance in this system. DFT calculations were used to assess the film-forming properties of these additives (Figure 8f). Results show that PES provides excellent film-forming properties. With minimal polarization increase during high-temperature cycling compared to MMDS, PES enhances the reversible lithium-ion intercalation/deintercalation and demonstrates superior high-temperature cycling and storage performance relative to MMDS.[48] Liu et al. discovered that VC and PES have beneficial effects on both the cathodes and anodes of lithium batteries. In a 1 M $LiPF_6$ with EC:DEC (v/v = 1 : 2) electrolyte, the compatibility of 2 % VC or 2 % PES with NMC622 is evaluated by accelerating capacity decay through

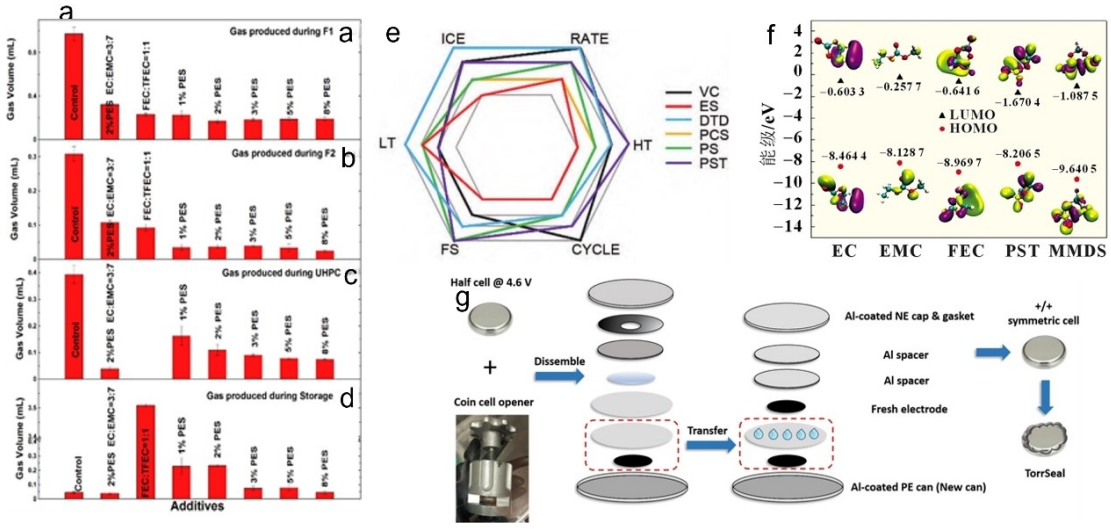

Figure 8. Volume of gas evolved during: (a) formation step 1; (b) formation step 2; (c) the 500 h storage at 40.0 ± 0.1 °C and (d) the 600 h UHPC cycle/store experiment at 40.0 ± 0.1 °C. Reproduced with permission.[46] Copyright 2016, Elsevier. (e) Performance radar chart of various electrolyte additives. (f) HOMO and LUMO of EC, EMC, FEC, PST and MMDS Molecular orbital energy level diagram. (g) Steps for building +/+ symmetric cells.

multiple voltage holding times at 55 °C. Electrochemical impedance spectroscopy (EIS) shows that 2% PES exhibits better impedance control (Figure 8g).[49]

2.5. 1,3-Propanediol Cyclic Sulfate (PCS)

1,3-propanediol cyclic sulfate (PCS), is transformed from the pentacyclic structure of DTD to a hexacyclic form, also serving as an additive to enhance cycling stability of high-voltage batteries. It not only forms a SEI film but also a CEI film, thus protecting both the cathodes and anodes. PCS can effectively suppress high-temperature gas generation, electrolyte decomposition, and lithium dendrite growth issues.

Liu et al. Studied PCS as a functional additive to enhance the cycling stability of $LiNi_{0.6}Co_{0.1}Mn_{0.3}O_2$/graphite cells. After adding 3.0 wt.% PCS to the baseline electrolyte, the capacity retention of the cell improves from 9.6% to 86.5% after 150 cycles at voltages ranging from 3.0 to 4.5 V. Based on theoretical calculations and characterization, the main reason for the enhanced electrochemical performance is that PCS forms a highly SEI/CEI layers on the electrodes surface (Figure 9a). These layers not only suppress electrolyte decomposition and increase interface impedance but also reduce the dissolution of transition metals. Therefore, PCS can be used as an additive in high-voltage electrolytes to improve practical applications.[50] Ding et al. studied the performance of DTD, PS, and PCS as electrolyte additives for lithium-ion batteries. DFT calculations show that DTD, PS, and PCS have relatively low lowest unoccupied molecular orbital (LUMO) energies and are more easily reduced on graphite anodes. CV curves, cycling performance, and AC impedance spectroscopy of lithium/graphite half-cells indicate that DTD and PCS are preferentially reduced to form stable SEI films. DTD, PS, and PCS can also reduce bubbles and gas expansion after battery high-temperature storage (Figure 9b).[51]

Kim et al. reported a sulfate additive added to thermally cross-linked gel-type polymer electrolyte (SA-TGPE), which consists of a PEO-based polymer matrix and PCS additive (Figure 9c). The sulfur-rich components formed by PCS in the lithium metal anode SEI layer contributes to the formation of a stable interface, ensuring uniform lithium deposition. Additionally, sulfur-rich components constitute a CEI layer that not only suppresses side reactions with transition metals but also enhances the oxidative stability of the PEO-based polymer in the electrolyte.[52] Felix et al. incorporated PCS into EC and electrochemical impedance spectroscopy confirmed that the addition of PCS results in a denser SEI layer. The inclusion of PCS can protectively modify the anode SEI layer, thereby inhibiting manganese oxide deposition (Figure 9d). As a novel sulfate-based additive, PCS performs well in high-voltage batteries by reducing capacity decay during cycling processes.[53] Xu et al. used tris(trimethylsilyl) phosphite (TMSP) and PCS as binary functional additives to address adverse reactions in high-voltage (5 V) $LiNi_{0.5}Mn_{1.5}O_4$/MCMB (graphite mesocarbon microbead) lithium-ion cells at room temperature and 50 °C. At room temperature, the high-voltage battery maintains a discharge capacity retention rate of 79.5% after 500 cycles at 0.5 C rate (Figure 9e). When the current intensity increased from 0.2 to 5 C, the discharge capacity retention rate with the binary functional additive is 90%. The characterizations confirm that the binary functional additive decomposes and participates in modifying the SEI layers on both electrodes. Due to synergistic effects, the SEI layers also exhibit conductive, protective, and oxidative stability properties against electrolyte oxidation/reduction reactions.[54] Xia et al. employed high-precision coulometry, AC impedance spectroscopy, and volume change measurements to infer gas evolution experiments of PCS additive used alone and in combination with 2% VC.

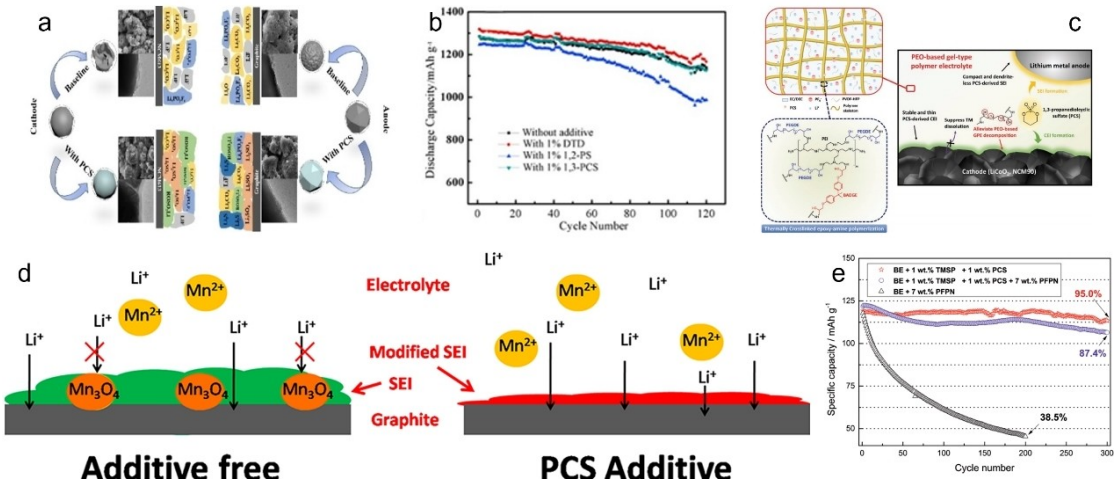

Figure 9. (a) The possible mechanism diagram of PCS additive working on electrode/electrolyte interface. Reproduced with permission.[50] Copyright 2023, Wiley. (b) cycling performance of $LiCoO_2$/graphite batteries. Reproduced with permission.[51] Copyright 2016, Elsevier. (c) A schematic illustration of the structure and epoxy-amine crosslinked polymerization of the SA-TGPE. Reproduced with permission.[52] Copyright 2023, Wiley. (d) Schematic diagram of SEI changes before and after adding PCS. Reproduced with permission.[53] Copyright 2013, the American Chemical Society. (e) The discharge capacity retention of the $LiNi_{0.5}Mn_{1.5}O_4$/MCMB full cells with BE, BE + binary functional additives, and BE + ternary functional additives at 1 C rate.

During the formation process, PCS significantly reduces irreversible capacity and gas evolution. However, when used alone, PCS cells exhibit far inferior performance in terms of Coulombic efficiency, capacity retention at charge endpoints, and voltage decay during storage compared to cells containing 2% VC.[55]

The summary about the test parameters and battery performances in the electrolytes containing monoester sultones have been listed in Table 1.

3. Bis-Sultones

3.1. Methylene Methanedisulfonate (MMDS)

Methylene methanedisulfonate (MMDS), a typical bis-sultone, have been widely used in high-voltage batteries. It can be preferentially oxidized to form an interfacial layer, promoting ion transport while inhibiting the decomposition of electrolyte solvents, maintaining the cycling stability of batteries, and enhancing the capacity retention of batteries.

Wang et al. proposed a mechanism for the expanded electrochemical stability window of MMDS electrolytes relative to traditional carbonate electrolytes based on molecular dynamics (MD) simulations and DFT calculations. Their team found that MMDS has stronger reduction capability and affinity for electrode surfaces compared to solvents, enabling MMDS to preferentially decompose and beneficially affect the SEI formation (Figure 10a). The use of MMDS reduces the likelihood of surface solvent ion complexes occurring during redox processes, suggesting its benefits for solvent stability.[56] Wang et al. developed a diethyl carbonate (DEC)-based electrolyte with MMDS as an additive. The MMDS additive in the electrolyte (3.38 V) preferentially oxidizes, effectively suppressing the generation of HF. In cycling performance tests, the addition of MMDS significantly improves the cell's cycling performance (Figure 10b). After storing fully charged (4.35 V) for 7 days, cells with added MMDS show improved stability performance. EIS, ICP, SEM, TEM, and XPS analyses indicate that MMDS forms a stable passivation film on the cathode, significantly hindering the dissolution of Mn from the $LiMn_2O_4$ electrode.[57] Zuo et al. studied the performance of MMDS as an electrolyte additive to relieve capacity decay of $LiCoO_2$/graphite lithium-ion cells (LIBs) during cycling within the 3.0–4.5 V range. LSV and cyclic voltammetry (CV) indicate that MMDS has a lower oxidation potential in a mixed solvent of EC and EMC, participating in the formation of the CEI film (Figure 10c). With 0.5 wt.% MMDS

Table 1. The test parameters and battery performances in the electrolytes containing monoester sultones.

	Voltages	Current densities	Capacities	Cycling stabilities
DTD	2.8–4.3 V	0.5 mA/cm^2	1.0 mAh/cm^2	95.8%/275 cycles
	2.8–4 V	2 C	337 mAh/g	90.5%/1000 cycles
	2.8–4 V	0.5 mA/g	1.23 mAh/g	81.4%/300 cycles
	2.5–4.2 V	0.3–1 C	4.32 Ah/g	80.72%/500 cycles
	3.0–4.3 V	1 C	215 mAh/g	80.72%/500 cycles
	3.0–4.3 V	1 mA/g	1.5 mAh/g	98%/20 cycles
	3.0–4.5 V	50 mA/g	177.81 mAh/g	92.29%/80 cycles
	2.8–4.2 V	C/2.2	220 mAh/g	95%/500 cycles
	3–4.95 V	29.4 mA/g	120 mAh/g	93%/300 cycles
	2.8–4.2 V	1 C	1000 mAh/g	85%/200 cycles
	3–4.2 V	0.2 A/g	882.2 mAh/g	80%/500 cycles
ES	3–4.6 V	105 mA/g	200 mAh/g	90%/200 cycles
	3–4.2 V	1 C	375 mAh/g	93%/160 cycles
	2.3–4.1 V	50 mA/g	203 mAh/g	95.2%/10000 cycles
	3–4.2 V	1 C	365 mAh/g	91%/150 cycles
1,3-PS	3–4.2 V	500 mA/g	1.18 Ah/g	98%/200 cycles
	3–4.3 V	1 C	168 mAh/g	95%/100 cycles
	3–4.3 V	1 C	200 mAh/g	85%/100 cycles
	2.75–4 V	1 C	500 mAh/g	82.7%/500 cycles
	3–4.1 V	1 C	130 mAh/g	75%/100 cycles
	3–4.5 V	1 C	196.3 mAh/g	89%/120 cycles
	3–4.5 V	1 C	180 mAh/g	85%/485 cycles
	0.05–2.5 V	0.4 mA/cm^2	357 mAh/g	100%/45 cycles
	3–5 V	0.5 C	600 mAh/g	80%/100cycles
	1.75–2.7 V	0.2 C	111 mAh/g	87%/100cycles
PES	3–4.2 V	1 C	140 mAh/g	85%/50 cycles
	3–4.4 V	12 mA/g	221 mAh/g	85%/500 cycles
	3–4.2 V	1 C	1530.1 mAh/g	94.1%/200 cycles
	2.5–4.2 V	0.1 C	138 mAh/g	91%/45 cycles
	2–3.8 V	80 mA/g	218 mAh/g	71%/1000 cycles
	3.5–4.9 V	1 C	123.2 mAh/g	90.8%/400 cycles
	2.75–4.2 V	1.8 A/g	3000 mAh/g	80%/1000 cycles
PCS	3–4.5 V	1 C	164.5 mAh/g	86.5%/150 cycles
	3–4 V	0.1 C	351 mAh/g	97.7%/50 cycles
	3–4.2 V	0.5 C	162.5 mAh/g	82.5%/200 cycles
	3.5–4.8 V	0.5 C	124.5 mAh/g	79.5%/500 cycles

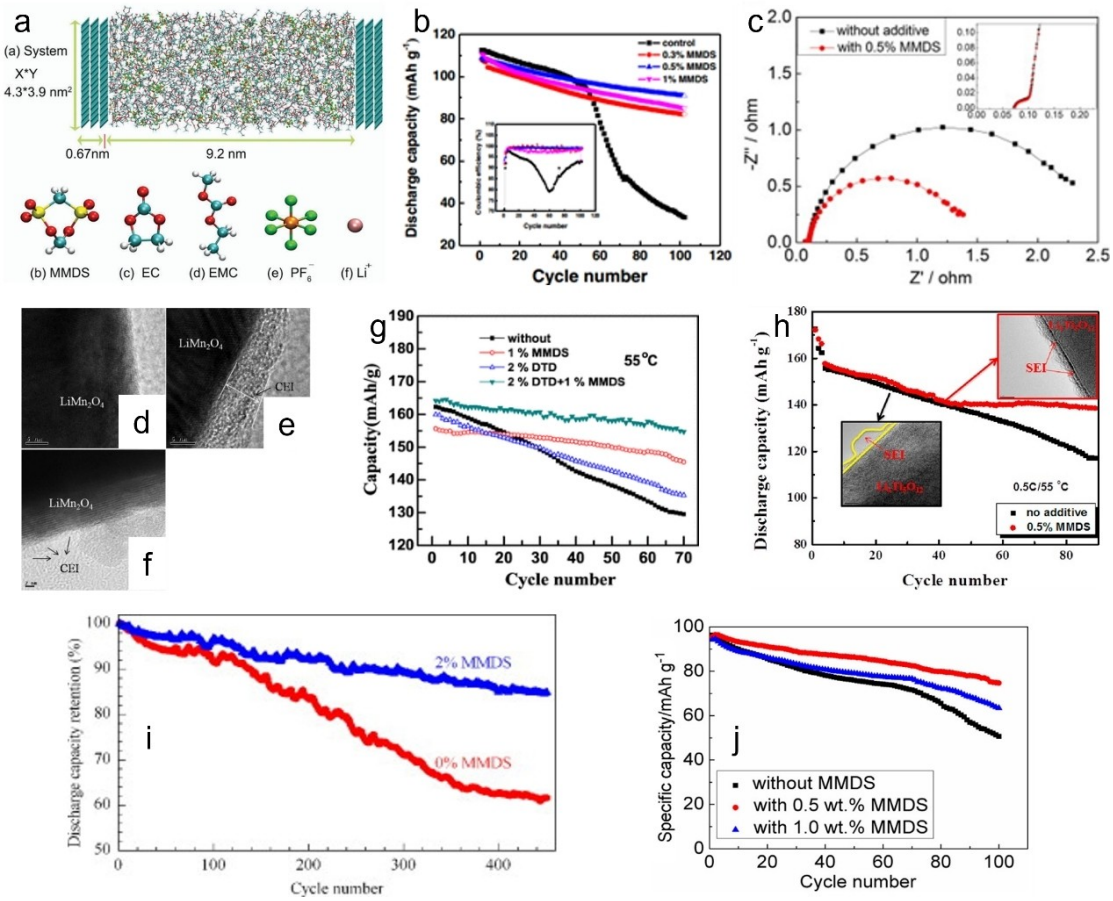

Figure 10. (a) Snapshot of the MMDS-containing electrolyte system and chemical structures of the electrolyte components. Reproduced with permission.[56] Copyright 2019, Royal Society of Chemistry. (b) Cycling performances of $LiMn_2O_4$/Li cells with different electrolytes at 55 °C between 4.35 and 3.0 V. Reproduced with permission.[57] Copyright 2015, Springer Link. (c) Electrochemical impedance spectra of $LiCoO_2$/graphite cells with and without MMDS charged to 4.5 V after 150 cycles. Reproduced with permission.[58] Copyright 2019, Elsevier. TEM micrographs of $LiMn_2O_4$ electrodes: (d) pristine electrode, and electrodes after 200 cycles at 55 °C using 1 M $LiPF_6$ in EC/DMC/EMC (1 : 1 : 1, wt.%) as electrolytes (e) without additive and (f) with 0.5 wt.% MMDS additive. Reproduced with permission.[59] Copyright 2014, Elsevier. (g) Cycle performance of the NCM111 in 1 M $LiPF_6$-EC:EMC electrolyte with different electrolyte under 55 °C. Reproduced with permission.[60] Copyright 2017, Springer Link. (h) Cyclic performance of $Li_4Ti_5O_{12}$/Li cells with and without MMDS additive cycled between 1 and 3 V at 55 °C. Reproduced with permission.[62] Copyright 2015, Elsevier. (i) Cycling performance of the $LiMn_2O_4$/graphite cell without MMDS and with 2 % MMDS in the electrolyte at 50 °C with a current rate of 0.5 C. Reproduced with permission.[63] Copyright 2014, Elsevier. (j) Cycle performance of $LiMn_2O_4$/graphite cells using different electrolytes at 60 °C. Reproduced with permission.[64] Copyright 2014, Elsevier.

added, the capacity retention of $LiCoO_2$/graphite cells increases significantly from 32.0 % to 69.6 % after 150 cycles at 3.0–4.5 V, and the rate capability also improved compared to cells without MMDS.[58]

Huang et al. investigated the impact of MMDS as an electrolyte additive to address the capacity fading of $LiMn_2O_4$ cathodes in lithium-ion cells (LIBs) under high-temperature cycling. By adding 0.5 wt.% MMDS to the electrolyte (1.0 M $LiPF_6$-EC/DMC/EMC), the capacity retention of $LiMn_2O_4$/Li cells significantly increases from 51.6 % to 72.8 % after 200 cycles at 55 °C. The MMDS additive can form a thin and conductive film on the $LiMn_2O_4$ surface, inhibiting oxidative decomposition of the electrolyte, enhancing SEI conductivity, and facilitating lithium-ion transport (Figure 10d–10f).[59] Cui et al. studied the electrochemical behavior of NCM111 in 1 M $LiPF_6$-EC electrolyte with DTD and MMDS additives, used individually or combined, at high cut-off voltages of 3.0–4.5 V at room temperature (25 °C) and high temperature (55 °C). Results indicate that MMDS reduces the initial discharge capacity of NCM111, but significantly enhances its long-cycle life, achieving a capacity retention of 99.23 % after 80 cycles at 4.5 V (Figure 10g). The optimal additive combination is 2 wt.% DTD + 1 wt.% MMDS, yielding a capacity retention of 102.2 % after 80 cycles at room temperature and 94.2 % after 70 cycles at 55 °C.[60] Xia et al. explored the effects of PS and MMDS as electrolyte additives, both alone and in combination with VC. When used individually, both additives reduce charge transfer resistance during cycling, with MMDS demonstrating better coulombic efficiency and lower charge endpoint capacity slippage than PS. The combination of MMDS and 2 % VC significantly improves coulombic efficiency and charge slippage rate, while reducing charge transfer resistance during cycling.[61]

Wang et al. investigated the performance of MMDS as an electrolyte additive to improve the cyclability of spinel lithium titanate ($Li_4Ti_5O_{12}$) lithium-ion cells. Linear sweep voltammetry (LSV) and electrochemical impedance spectroscopy (EIS) show that MMDS participates in the formation of the SEI above 1 V. A stable SEI film on the surface of $Li_4Ti_5O_{12}$ is considered as the

most effective barrier layer to inhibit interfacial reactions and gas generation (Figure 10h). Adding 0.5 wt.% MMDS to the electrolyte significantly improveds the cycling performance of $Li_4Ti_5O_{12}$/Li cells.[62] Bian et al. studied the effect of MMDS on the high-temperature (50 °C) cycling performance of $LiMn_2O_4$/graphite cells. The results show that the addition of 2 wt.% MMDS to conventional electrolyte significantly improves the high-temperature cycling performance of $LiMn_2O_4$/graphite cells. MMDS can participate in the formation of SEI films on both the $LiMn_2O_4$ cathode and graphite anode, resulting in increased polarization and initial specific capacity decrease (Figure 10i).[63] Zuo et al. also investigated MMDS as an electrolyte additive for $LiMn_2O_4$ cathodes to enhance thermal stability. Cells using 1.0 M $LiPF_6$-EC/EMC/DMC (1 : 1 : 1) with 0.5 wt.% MMDS retain 79.2 % of their initial capacity after 100 cycles at 60 °C, compared to only 52.7 % for cells without the additive. After storage at 85 °C for 24 hours, cells with 0.5 wt.% MMDS show a discharge capacity retention of 82.5 %, still higher than the 71.8 % of cells without MMDS (Figure 10j).[64]

3.2. [4,4′-Bis(1,3,2-Dithiazolidine)] 2,2′-Dioxide (BDTD)

[4,4′-bis(1,3,2-dithiazolidine)] 2,2′-dioxide (BDTD), formed by two ES molecules, has the capability to create a stable film that prevents impedance increase and lithium dendrite growth, making it a suitable additive for high-voltage conditions, thereby extending battery life.

Lee et al. studied BDTD as a novel electrolyte additive to enhance the electrochemical performance of NMC532 cathodes in the voltage range of 3.0–4.6 V. XPS and EIS of cells indicate that BDTD preferentially oxidizes over electrolyte solvents, forming a stable film on the cathode surface, which prevents impedance increase caused by electrolyte solvent decomposition at high voltages. Adding a small amount of BDTD to 1.0 M $LiPF_6$/EC/EMC (3 : 7 by volume) electrolyte can improve the cycling performance of the cells (Figure 11a). Therefore, BDTD is a promising new additive for high-voltage conditions.[65]

Jinsol et al. developed a novel sulfite-based electrolyte additive BDTD and applied it in high-voltage lithium metal batteries (LMB). SEM images show that BDTD can suppress lithium dendrite growth on the lithium metal anode. Additionally, XPS results confirm the stability of the cathode-electrolyte interface formed by the BDTD additive on the $LiNi_{0.6}Mn_{0.2}Co_{0.2}O_2$ cathode (Figure 11b–11f). BDTD can synergistically enhance both electrodes, thus extending high-capacity retention life under high-voltage operation (4.6 V).[66]

3.3. [4,4-Bi(1,3,2-Dioxathiolane)] 2,2,2,2-Tetraoxide (BDTT)

[4,4-bi(1,3,2-dioxathiolane)] 2,2,2,2-tetraoxide (BDTT), formed by the combination of two DTD molecules, is a novel cathode-

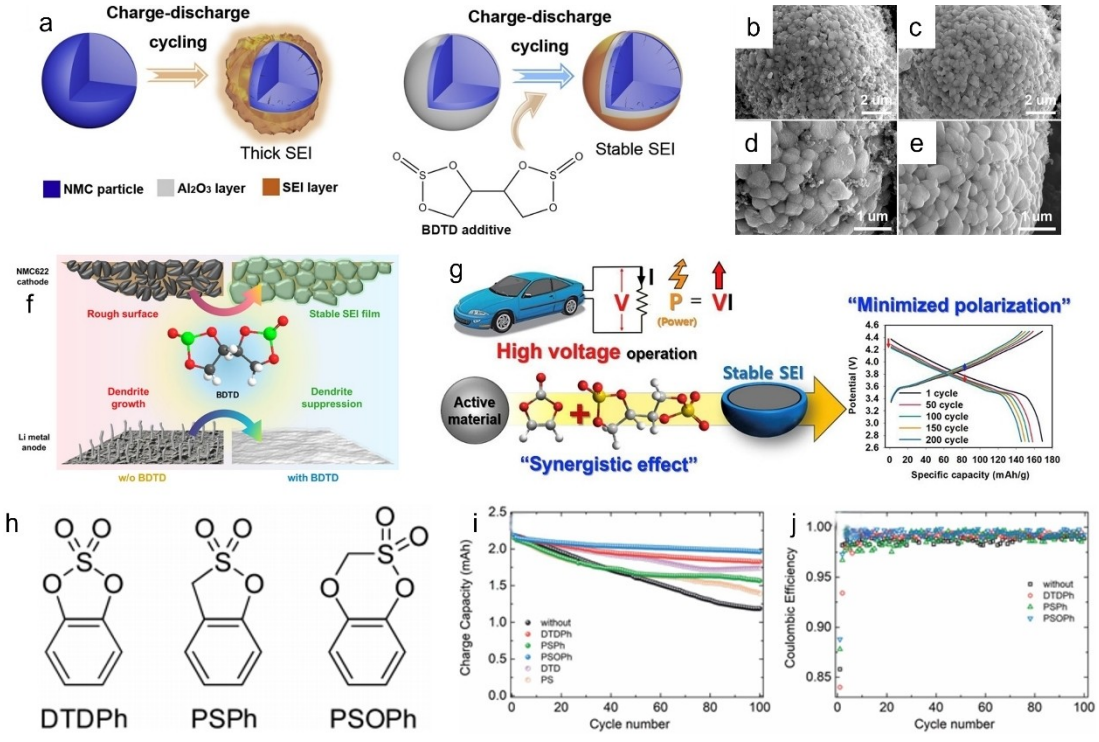

Figure 11. (a) The proposed machanism of BDTD additives. Reproduced with permission.[65] Copyright 2018, Elsevier. Surface SEM images of NMC622 cathode. (b,d) w/o and (c,e) w/BDTD after 100th cycling of NMC622/Li cell. (f) Schematic illustrations of the dual-function mechanism of BDTD additive on the surfaces of the Li metal anode and the NMC622 cathode. Reproduced with permission.[66] Copyright 2021, Elsevier. (g) The conceptual image of synergistic effect of dual additives and voltage profiles at a current density rate of 0.5 C of the NMC532/graphite full cells with mixture of the two additives. Reproduced with permission.[67] Copyright 2019, Elsevier. (h) Chemical structures of the additives. Cycling of full-cells at C/10 rate without/with 1 wt.% of additive: cycling performance (i) and corresponding coulombic efficiency (j). Reproduced with permission.[68] Copyright 2018, Royal Society of Chemistry.

stabilizing additive that can create a CEI layer, protecting the cathode during high-voltage cycling.

Lithium batteries typically suffer from severe and persistent electrolyte decomposition and electrode surface instability during high-voltage cycling. Park et al. used the BDTT as a novel cathode stabilizing additive for the first time, combined with the anode stabilizing additive VC, to enhance the electrochemical performance of $LiNi_{0.5}Mn_{0.3}Co_{0.2}O_2$/graphite full cells. The synergistic effect of the dual cathode and anode stabilizers leads to high capacity and a retention rate of 86% over 200 cycles (Figure 11g).[67]

3.4. 1,3,2-Benzodioxathiole2,2-Dioxide (DTDPh)

1,3,2-benzodioxathiole2,2-dioxide (DTDPh), is a derivative with a benzene ring added to DTD or PS, serving as an aromatic ring derivative. The SEI films formed by these substances have lower reduction resistance and higher reduction stability in high-voltage batteries.

Jankowski et al. presented the concept of chemically soft SEI-forming additives. This strategy entails the modification of established SEI-formers through the incorporation of aromatic ring-based derivatives, thereby enhancing their chemical softness. Consequently, this methodology has yielded compounds such as 1,3,2-benzodioxathiole 2,2-dioxide (DTDPh), 3H-1,2-benzoxathiole 2,2-dioxide (PSPh), and 1,4,2-benzodioxathiine 2,2-dioxide (PSOPh). Comparison in conjunction with DFT predicts prospects for both early and controlled reduction processes (Figure 11h). The SEI layer formed with PSOPh especially demonstrates excellent performance in improving capacity retention, enhancing coulombic efficiency, and reducing resistance. This is due to the preferred C–O bond breaking mechanism, supported by the S–C bond breaking mechanism, which together result in a SEI layer with good conductivity and adhesion properties. The addition of an aromatic ring to the SEI-forming additive provides lower anti-reduction properties and higher reduction stability. The presence of the aromatic ring offers good adhesion to the graphite electrode, while the high oxygen content ensures high lithium-ion conductivity and low resistance (Figure 11i and 11j).[68]

3.5. 1,2,6-Oxadithiane 2,2,6,6-Tetraoxide (ODTO)

1,2,6-oxadithiane 2,2,6,6-tetraoxide (ODTO), possessing a structural similarity to MMDS, can convert into sulfur-containing substances on the surfaces of both electrodes, forming SEI/CEI interfacial layers and thus protecting both electrodes simultaneously.

Ma et al. evaluated the use of ODTO as a novel electrolyte additive in both coated and uncoated single-crystal $Li[Ni_{0.5}Mn_{0.3}Co_{0.2}]O_2$/graphite pouch cells. ODTO exhibits a structure closely resembling that of MMDS, yet demonstrates superior battery performance compared to MMDS. ODTO effectively passivates the graphite anode at 1.4 V and facilitates the formation of a SEI layer at the cathode. XPS analysis of cells containing 1% ODTO reveals that ODTO predominantly converts into sulfur-containing species on the surfaces of both electrodes. Ultra-high precision coulometry (UHPC) and long-term cycling show that only 3% ODTO can significantly enhance CE and result in high capacity retention in both uncoated and coated cells. Cells utilizing uncoated NMC532 in conjunction with an additive mixture of 1% ODTO, 1% $LiPO_2F_2$, 2% VC, or 2% FEC exhibit comparable cycling performance to those employing coated NMC532 with the same electrolyte composition. This suggests that coating the NMC532 is superfluous when efficacious additives are incorporated.[69]

The summary about the test parameters and battery performances in the electrolytes containing bis-sultones have been listed in Table 2.

4. Side-Chain Sulfones

4.1. 3-Fluoro-1,3-Propane Sultone (FPS)

3-fluoro-1,3-propane sultone (FPS), possessing an additional fluorine group compared to PS, functions as an electron-withdrawing group, rendering FPS more readily reducible than other additives. This characteristic imparts a robust SEI-forming capability, enhancing anode stability and resistance to degradation at elevated temperatures, thereby establishing FPS as an exceptional electrolyte additive.

Table 2. The test parameters and battery performances in the electrolytes containing bis-sultones.

	Voltages	Current densities	Capacities	Cycling stabilities
MMDS	3–4.3 V	1 C	112 mAh/g	84%/100 cycles
	3–4.2 V	130 mA/g	120 mAh/g	85%/450 cycles
	3–4.3 V	1 C	110 mAh/g	91.8%/200 cycles
	3–4.5 V	50 mA/g	177 mAh/g	99.2%/80 cycles
	1–3 V	0.5 C	170 mAh/g	87%/85 cycles
	3–4.5 V	0.5 C	179.5 mAh/g	70%/150 cycles
	2.7–4.5 V	1 C	98.9 mAh/g	85.9%/200 cycles
BDTD	3–4.6 V	1 C 0.5 C	189 mAh/g198 mAh/g	91.6%/100 cycles
	2.7–4.6 V			97.3%/100 cycles
BDTT	2.7–4.5 V	0.5 C	169.3 mAh/g	88.7%/200 cycles
DTDph	2.6–3.8 V	0.1 C	189 mAh/g	97%/100 cycles
ODTO	3–4.3 V	C/3	226 mAh/g	97.6 %/200 cycles

Jung et al. proposed FPS as a novel SEI additive to supplant VC and PS. DFT calculations and electrochemical experiments confirm that the electron-withdrawing fluorine group significantly enhances anode stability and SEI formation capability. FPS exhibits markedly enhanced cycling performance compared to PS and surpasses the performance of VC in $LiCoO_2$/graphite cells across a broad temperature range (25–60 °C). During high-temperature storage at 90 °C, cells containing VC experience significant swelling, whereas those incorporating FPS effectively mitigate thermal degradation (Figure 12a and 12b). Therefore, FPS demonstrates high anode stability, exceptional cyclability, and robust thermal stability, establishing it as an outstanding SEI additive for enhancing the performance of contemporary lithium-ion batteries (Figure 12c).[70]

Han et al. conducted calculations on the HOMO, LUMO, and binding energies of 33 organic molecules with Li^+ ions, which serve as electrolyte additives for SEI formation in lithium batteries. Based on their calculations, they identified five SEI-forming additives exhibiting anode stability comparable to that of FPS: (4) fluoroethylene carbonate, (5) trifluoromethyl propylene carbonate, (12) methyl chloroformate, (18) butane sultone, (32) chloroethylene carbonate.[71]

4.2. Vinyl Ethylene Sulfite (VES)

Vinyl ethylene Sulfite (VES), synthesized from ES by the addition of an ethylene group, functions as a sultones capable of being reduced to form a dense SEI layer, thereby improving the cycling performance, rate capability, and high-temperature performance of high-voltage batteries.

Yao et al. investigated VES as a novel additive for PC-based lithium-ion battery electrolytes. Electrochemical results indicate that the addition of an appropriate amount of VES to the PC-based electrolyte significantly enhances the electrochemical performance of graphite materials (Figure 12d–12f). This enhancement is attributed to the reduction of VES, forming a dense SEI layer that prevents the intercalation of PC molecules. Spectroscopic results reveal that VES can be reduced to $ROSO_2Li(R{=}C_4H_6)$, Li_2SO_3, and butadiene (C_4H_6) before the decomposition of PC. Some Li_2SO_3 can undergo further reduction to form Li_2S and Li_2O, all of which are confirmed to be components of the SEI layer (Figure 12g and 12 h).[72]

The summary about the test parameters and battery performances in the electrolytes containing side-chain sultones have been listed in Table 3.

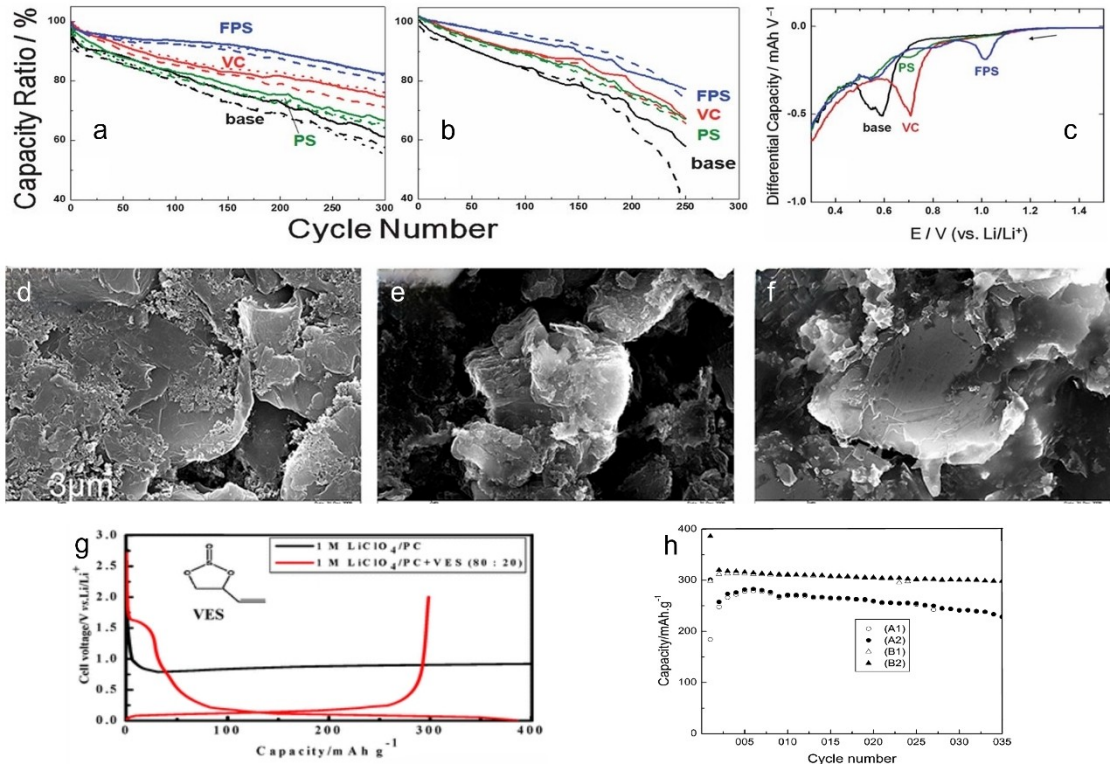

Figure 12. Cycle performance of $LiCoO_2$/graphite pouch cells with 1 M $LiPF_6$ EC/EMC (1/2, v/v) solutions with no additive and 2 wt.% of each additive (a) at 25 °C and (b) at 45 °C. (c) Differential capacity (dQ/dV) curves of graphite/Li coin cells with 1 M $LiPF_6$ EC/EMC (1/2 v/v) solutions with no additive and 2 wt.% of each additive. Reproduced with permission.[70] Copyright 2013, Royal Society of Chemistry. SEM images of CAG electrode surface obtained (d) before charging, (e) after charging for ten hours in 1 M $LiClO_4$/PC, and (f) after the first charge to 0.005 V in 1 M $LiClO_4$/PC + VES (80:20). (g) The first charge/discharge voltage profiles of the CAG/Li half-cell in 1 M $LiClO_4$/PC electrolytes with different volume content of VES cycled between 2.0–0.005 V at 37 mA g^{-1} and current density. (h) Cycle performances of CAG/Li cells in two kinds of electrolytes, (A_1) and (A_2) 1 M $LiClO_4$/PC + VES (90:10), (B_1) and (B_2) 1 M $LiClO_4$/ PC + VES (80:20). Reproduced with permission.[72] Copyright 2009, Royal Society of Chemistry.

5. Summary and Outlook

5.1. Summary

With the development of EVs and HEVs, the demand for high output power and endurance of lithium batteries continues to increase, and correspondingly the requirements for battery energy density continue to increase. In addition to choosing high energy cathode materials, it is also an effective way to improve energy density by making the power battery work at high voltage. The performance of high-voltage lithium batteries is mainly determined by the structure and performance of their electrode materials and electrolytes, of which electrolytes are very important. In general, with the increase of energy density, the compaction density of cathodes and anodes will increase, the insertion ability of electrolyte will become worse, and the retention rate of the liquid will be reduced, resulting in poor cycling and storage performance in the battery. In high voltage operating environments, there will be higher requirements for the electrolyte of power battery, so some special electrolytes with better oxidation resistance are needed. The electrolyte is often called the blood of the lithium battery, for one thing, the electrolyte is the bridge between the cathodes and anodes; Second, it is also a transport medium for ion migration. It is well known that additives are crucial to the development of high voltage electrolyte systems, and the solvation structure of the electrolyte can be changed by introducing some additives.

Since 1996, sultones have been reported in the literatures as electrolyte additives. Because the sulfonic acid groups in the electrolyte can preferentially reduce and decompose to form an excellent SEI layer, they play an important role in the insertion ability of the electrolyte, the liquid retention rate, the transmission ability of lithium ions, and the protection ability of the solvent. In this review, all the sultones reported have excellent modification of high voltage or high temperature batteries based on their SEI/CEI formation ability, which can protect the solvent from decomposition under high voltage conditions, inhibit the formation of lithium dendrites and improve the battery life, and promote the insertion and migration cycle of lithium ions in the electrode, and improve the capacity retention rate under high voltage conditions. Therefore, this series of sultones can be used as a high voltage electrolyte to improve the performance of the battery, are particularly good high voltage electrolyte additives.

In addition, the HOMO and LUMO values of electrolyte additives are important indicators to confirm the REDOX capacities. Among them, HOMO means the highest occupied molecular orbital, and LUMO represents the lowest unoccupied molecular orbital. It is worthy noting that the higher the HOMO value of the molecule, the easier it is to be oxidized on the cathode, and meanwhile the lower the LUMO value of the molecule, the easier it is to be reduced at the anode. The summaries about the LUMO and HOMO levels of sultone electrolyte additives have been listed in Table 4.

Table 4. The LUMO and HOMO levels of sultone electrolyte additives.

	LUMO	HOMO
DTD	−2.7879 eV	−7.99 eV
ES	0.002 eV	−8.413 eV
1,3-PS	−0.043 eV	−8.826 eV
PES	−1.67 eV	−8.2072 eV
PCS	−1.13 eV	−7.46 eV
MMDS	−1.497 eV	−9.64 eV
BDTD	21.448 eV	−4.809 eV
BDTT	17.372 eV	−7.23 eV
DTDph	−0.19 eV	−8.62 eV
FPS	0.29 eV	−8.75 eV
VES	−0.0471 eV	−0.2945 eV

5.2. Outlook

Electrolyte is one of the four key components of lithium battery (cathode, anode, diaphragm and electrolyte), known as the blood of lithium battery, so its performance directly restricts the development of lithium battery. Here, some views are put forward on the development trend of high voltage electrolytes in the future: (1) Mobile digital product batteries: focusing on the development of new solvents with high voltage and high boiling point, to prevent the decomposition of solvents under high charge termination voltage, and also need to add high voltage additives to increase the cycle life of the battery; (2) Electric vehicle power batteries: focusing on the development of new solvents with good thermal stability; Development of anti-overcharge additives with excellent high temperature performance, and more stable and durable electrolytes for fast charging under high pressure; (3) Military large-capacity batteries: focusing on the development of new solvents with low melting point and low viscosity; The development of new SEI/CEI formation additives can reduce the impedance of SEI/CEI and improve the mobility of lithium ions; And the development of safety additives with low temperature properties. In the future, the working environment of high-voltage batteries will be normalized, and with the emergence of ultra-high voltage overcharge and energy supplement technology, the performance requirements of batteries in high-voltage environments

Table 3. The test parameters and battery performances in the electrolytes containing side-chain sultones.

	Voltages	Current densities	Capacities	Cycling stabilities
FPS	3–4.2 V	0.1 C	1350 mAh/g	82%/300 cycles
VES	3–4 V	0.1 C	301 mAh/g	98%/35 cycles

will be an important development direction, so high-voltage electrolyte will become a research hotspot.

Additionally, sultones can be also used in sodium-ion batteries, potassium-ion batteries, lithium-sulfur batteries, and solid batteries.They can not only exhibit high oxidation resistance and create a stable protective layer on the electrode surface, but also effectively promote uniform anionic and cationic flux and inhibit dendrite growth.[73,76] Some sultones molecules, such as PS, PST, etc., are currently banned in Europe and the United States owing to their toxicity. However, there are some alternatives, such as BS, BST, etc., which have the same functions.[77,78]

Acknowledgements

This work was financially supported by the National Natural Science Foundation of China (No. 21978073 and U1903217), Hubei Key Research and Development Projects of China (No. 2023BAB148), Wuhan Knowledge Innovation Special Project and Innovation and Development Joint Fund of Hubei Natural Science (No. 2022CFD113).

Conflict of Interest

The authors declare no conflict of interest.

Keywords: Sultones · High voltage · Lithium batteries

[1] Y. S. Meng, V. Srinivasan, K. Xu, *Science* **2022**, *378*, 6624.
[2] S. Wan, W. Ma, Y. Xiao, S. M. Chen, *Batteries & Supercaps* **2022**, *5*, e202200368.
[3] M. Palluzzi, A. Tsurumaki, N. Mozhzhukhina, J. Rizell, A. Matic, P. Dangel, A. Navara, *Batteries & Supercaps* **2024**, *7*, e202400068.
[4] J. H. Wang, Y. K. Yamada, K. Sodeyama, C. H. Chiang, Y. Tateyama, A. Yamada, *Nat. Commun.* **2016**, *7*, 12032.
[5] Q. F. Zheng, Y. Yamada, R. Shang, S. Ko, Y. Y. Lee, K. Kim, E. Nakamura, A. Yamada, *Nat. Energy* **2020**, *5*, 291–298.
[6] S. P. Li, S. Fang, Z. W. Li, W. Y. Chen, H. Dou, X. G. Zhang, *Batteries & Supercaps* **2022**, *5*, e202100416.
[7] Y. X. Huang, Y. X. Xie, M. L. Sun, H. Chen, P. Dai, S. S. Liu, C. Y. Ouyang, C. Y. Liu, B. B. Hu, S. J. Liao, L. Huang, S. G. Sun, *ACS Sustain. Chem. & Eng* **2023**, *11*, 3760–3768.
[8] Y. Hu, Z. H. Zhang, H. M. Wang, *ChemistrySelect* **2022**, *7*, e202200740.
[9] F. H. Meng, S. Zhu, J. H. Gao, F. Z. Zhang, D. W. Li, *Ionics* **2021**, *27*, 3821–3827.
[10] F. Q. An, H. L. Zhao, W. N. Zhou, Y. H. Ma, P. Li, *Sci. Rep.* **2019**, *9*, 14108.
[11] T. Taskovic, L. M. Thompson, A. Eldesoky, M. D. Lumsden, J. R. Dahn, *J. Electro. Chem. Soc.* **2021**, *168*, 010514.
[12] S. L. Glazier, J. Li, X. W. Ma, L. D. Ellis, J. P. Allen, Kevin L. Gering, J. R. Dahn, *J. Electro. Chem. Soc* **2018**, *165*, A867–A875.
[13] Y. L. Cui, C. Yang, Z. H. Zhuang, M. Z. Wang, Q. C. Zhuang, *J. Inorg. Organomet. Polym* **2018**, *28*, 731–737.
[14] D. Y. H. Wang, J. R. Dahn, *J. Electrochem. Soc* **2014**, *161*, A1890–A1897.
[15] Z. Y. Yu, M. H. Bai, B. Hong, Y. Q. Lai, Y. X. Liu, *Ionics* **2022**, *28*, 4095–4101.
[16] D. X. Ouyang, K. Wang, T. F. Gao, Z. R. Wang, in 2022 *J. Loss. Prevent. Proc*80, p. 104924.
[17] J. Ming, Z. Gao, Y. Q. Wu, W. Wahyudi, W. X. Wang, X. R. Guo, L. Cavallo, J. Y. Hwang, A. Shamim, L. J. Li, Y. K. Sun, H. N. Alshareef, *ACS Energy Lett* **2019**, *4*, 2613–2622.
[18] W. J. Zhang, S. M. Yang, S. Heng, X. M. Gao, Y. Wang, W. X. Zhang, Q. T. Qu, H. H. Zheng, *Funct. Mater. Lett.* **2020**, *13*, 2051041.
[19] X. Zheng, Y. Liao, Z. R. Zhang, J. P. Zhu, F. C. Ren, H. J. He, Y. X. Xiang, Y. Z. Zheng, Y. Yang, *J. Energy. Chem* **2020**, *42*, 62–70.
[20] B. Han, Y. C. Zou, G. Y. Xu, S. Q. Hu, Y. Y. Kang, Y. X. Qian, J. Wu, X. M. Ma, J. Q. Yao, T. T. Li, Z. Zhang, H. Meng, H. Wang, Y. H. Deng, J. Li, M. Gu, *Energy Environ. Sci.* **2021**, *14*, 4882.
[21] M. M. Fang, J. E. Chen, B. Y. Chen, J. H. Wang, *J. Mater. Chem. A* **2022**, *10*, 19903.
[22] K. Zhou, H. H. Yang, J. H. Zhou, Y. Tian, J. W. Guo, M. H. Yuan, L. B. Liu, L. G. Gui, *Electrochim. Acta* **2023**, *462*, 142768.
[23] P. L. Wang, X. Z. Sun, Y. B. An, X. Zhang, C. Z. Yuan, S. H. Zheng, K. Wang, Y. W. Ma, *Rare Met.* **2022**, *41*, 1304–1313.
[24] N. Matsuoka, H. Kamine, Y. Natsume, A. Yoshino, *ChemElectroChem* **2021**, *8*, 3095–3104.
[25] K. Suzuki, S. Sawayama, Y. Deguchi, R. Sai, J. Han, K. Fuji, *Phys. Chem. Chem. Phys.* **2022**, *24*, 27321.
[26] D. W. Xu, Y. Y. Kang, J. Wang, S. G. Hu, Q. Shi, Z. G. Lu, D. S. He, Y. F. Zhao, Y. X. Qian, H. M. Lou, Y. H. Deng, *J. Power Sources* **2019**, *437*, 226929.
[27] F. W. Lin, Ngoc Thanh Thuy Tran, W. D. Hsu, *ACS Omega* **2020**, *5*, 13541–13547.
[28] J. M. Oh, J. M. Kim, Y. M. Lee, J. Y. Kim, D. Ok Shin, My. J. Lee, S. B. Hong, Y. G. Lee, Kw. M. Kim, *Mater. Res. Bull* **2020**, *132*, 111008.
[29] T. Yim, S. H. Kim, S. G. Woo, Ky. J, Lee, J. H, Song, W. S, Cho, K. J, Kim, J. S, Kim, Y. J, Kim, *RSC Adv.* **2014**, *4*, 19172.
[30] X. X. Li, L. Liu, S. M. Li, L. Guo, B. Li, G. Q. Zhang, *Front. Mater.* **2020**, *7*, 263.
[31] M. Q. Xu, W. S. Li, B. L. Lucht, *J. Power Sources* **2009**, *193*, 804–809.
[32] M. Hekmatfar, L. Hasa, R. Eghbal, D. V. Carvalho, A. Moretti, S. Passerini, *Adv. Mater. Interfaces* **2020**, *7*, 1901500.
[33] A. Birrozzi, N. Laszczynski, M. Hekmatfar, J. V. Zamory, G. A. Giffin, S. Passerini, *J. Power Sources* **2016**, *325*, 525–533.
[34] J. Pires, L. Timperman, A. Castets, J. S. Pena, E. Dumont, S. Levasseur, R. Dedryvere, C. Tessier, M. Anounti, *RSC Adv.* **2015**, *5*, 42088.
[35] B. Zhang, M. Metzger, S. Solchenbach, M. Payne, S. Meini, H. A. Gasteiger, A. Garsuch, B. L. Lucht, *J. Phys. Chem. C* **2015**, *119*, 21, 11337–11348.
[36] G. Park, H. Nakamura, Y. S. Lee, M. Yoshio, *J. Power Sources* **2009**, *189*, 602–606.
[37] H. Lee, S. Choi, S. H. Choi, H. J. Kim, Y. S. Choi, S. J. Yoon, J. J. Cho, *Electrochem. Commun* **2007**, *9*, 801–806.
[38] J. H. Kim, S. Y. Bae, J. H. Min, S. W. Song, D. W. Kim, *Electrochim. Acta* **2012**, *78*, 11–16.
[39] M. Zhou, X. M. Wang, Y. N. Yuan, Z. Cao, H. H. Zheng, *Bat. Bimon* **2022**, *52*, 1001–1579.
[40] B. Li, M. Q. Xu, T. T. Li, W. S. Li, S. J. Hu, *Electrochem. Commun* **2012**, *17*, 92–95.
[41] L. Ma, J. Xia, J. R. Dahn, *J. Electrochem. Soc* **2014**, *161*, A2250–A2254.
[42] B. Li, Y. Q. Wang, W. Q. Tu, Z. S. Wang, Z. S. Wang, M. Q. Xu, L. D. Xing, W. S. Li, *Electrochim. Acta* **2014**, *147*, 636–642.
[43] B. Li, M. Q. Xu, B. Z. Li, Y. L. Liu, L. Yang, W. S. Li, S. J. Hu, *Electrochim. Acta* **2013**, *105*, 1–6.
[44] W. F. Song, B. Hong, S. Hong, Y. Q. Lai, J. Li, Y. X. Liu, *Int. J. Electrochem. Sci* **2017**, *12*, 10749–10762.
[45] J. Xia, L. Ma, J. R. Dahn, *J. Power Sources* **2015**, *287*, 377–385.
[46] J. Xia, M. Nie, J. C. Burns, A. Xiao, W. M. Lamanna, J. R. Dahn, *J. Power Sources* **2016**, *307*, 340–350.
[47] H. H. Xia, P. C. Liang, Z. X. Ah, *Energy Storage Sci, Tech* **2023**, *12*, 2391–2440.
[48] S. Q. Qiao, H. Yang, C. S. Sun, Y. J. Guo, *Power Technology* **2023**, *147*, 298–301.
[49] Y. L. Liu, I. Hamam, J. R. Dahn, *J. Electrochem. Soc.* **2020**, *167*, 110527.
[50] S. Liu, W. J. Qiu, Z. Y. Su, J. Li, X. Xiao, J. M. Nan, X. X. Zuo, *ChemElectroChem* **2023**, *10*, e202201039.
[51] Z. Y. Ding, X. C. Li, T. Wei, Z. L. Yin, X. H. Li, *Electrochim. Acta* **2016**, *196*, 622–628.
[52] S. H. Kim, N. J. Park, W. B. Lee, J. H. Park, *Small* **2024**, *20*, 2309160.
[53] F. Lix, J. H. Cheng, S. Hy, John Rick, F. M. Wang, B. J. Hwang, *J. Phys. Chem. C* **2013**, *117*, 22619–22626.
[54] G. J. Xu, C. G. Pang, B. B. Chen, J. Ma, X. Wang, J. C. Chai, Q. F. Wang, W. Z. An, X. H. Zhou, G. L. Cui, L. Q. Chen, *Adv. Energy Mater.* **2018**, *8*, 1701398.
[55] J. Xia, R. Petibon, N. N. Sinha, J. R. Dahn, *J. Electrochem. Soc* **2015**, *162*, 2227–2235.
[56] Y. M. Wang, X. Y. Yu, Y. C. Liu, Q. Wang, *Phys. Chem. Chem. Phys* **2019**, *21*, 217.

[57] R. H. Wang, X. H. Li, Z. X. Wang, H. J. Guo, *J. Solid State Electrochem* **2016**, *20*, 19–28.
[58] X. X. Zuo, C. J. Fan, X. Xiao, J. S. Liu, J. M. Nan, *J. Power Sources* **2012**, *219*, 94–99.
[59] T. Huang, M. X. Wu, W. G. Wang, Y. Pan, G. H. Fang, *J. Power Sources* **2014**, *262*, 303–309.
[60] Y. L. Cui, C. Yang, Z. H. Zhuang, M. Z. Wang, Q. C. Zhuang, *J. Inorg. Organomet. Polym* **2018**, *28*, 731–737.
[61] J. Xia, J. E. Harlow, R. Petibon, J. C. Burns, L. P. Chen, J. R. Dahn, *J. Electrochem. Soc* **2014**, *161*, 547–553.
[62] R. H. Wang, X. H. Li, B. Zhang, Z. X. Wang, H. J. Guo, *J. Alloy. Compd* **2015**, *648*, 512–520.
[63] F. J. Bian, Z. R. Zhang, Y. Yang, *J. Energy Chem* **2014**, *23*, 383–390.
[64] X. X. Zuo, J. H. Wu, C. J. Fan, K. Lai, J. S. Liu, J. M. Nan, *Electrochim. Acta* **2014**, *130*, 778–784.
[65] S. H. Lee, S. K. Yoon, E. H. Hwang, Y. G. Kwon, Y. G. Lee, K. Y. Cho, *J. Power Sources* **2018**, *378*, 112–118.
[66] J. Im, J. Ahn, H. J. Choi, Y. G. Lee, S. K. Yoon, K. Y. Cho, *J. Alloy. Compd.* **2021**, *872*, 159662.
[67] E. J. Park, Y. G. Kwon, S. K. Yoon, K. Y. Cho, *J. Power Sources* **2019**, *441*, 126668.
[68] P. Jankowski, M. Poterata, N. Lindahl, W. Wieczorek, P. Johansson, *J. Mater. Chem. A* **2018**, *6*, 22609.
[69] X. W. Ma, R. S. Young, L. D. Ellis, L. Ma, J. Li, J. R. Dahn, *J. Electrochem. Soc* **2019**, *166*, 2665–2672.
[70] H. M. Jung, S. H. Park, J. H. Jeon, Y. S. Choi, S. J. Yoon, J. J. Cho, S. Oh, S. W. Kang, Y. K. Han, H. Lee, *J. Mater. Chem. A* **2013**, *1*, 11975–11981.
[71] Y. K. Han, K. Lee, S. C. Jung, Y. S. Huh, *Comput. Theor. Chem* **2014**, *1031*, 64–68.
[72] W. H. Yao, Z. R. Zhang, J. Gao, J. Li, J. Xu, Z. C. Wang, Y. Yang, *Energy Environ. Sci* **2009**, *2*, 1102–1108.
[73] H. R. Cheng, Z. Ma, P. P. Kumar, H. H. Liang, Z. Chao, Q. Li, J. Min, *ACS Energy Lett.* **2024**, *4*, 1604–1616.
[74] J. Chen, Z. Yang, X. Xu, Y. Qiao, Z. M. Zhou, Z. Q. Hao, X. M. Chen, Y. Liu, X. Q. Wu, X. Z. Zhou, L. Li, S. L. Chou, *Adv. Mater.* **2024**, *36*, 2400169.
[75] H. M. Zhao, J. X. Qi, J. C. Zhou, Q. D. Tao, E. M. Li, B. H. Dai, J. J. Huang, T. M. Lu, J. Li, *Energy Fuels* **2024**, *15*, 14663–14671.
[76] J. Wu, H. Y. Qiu, J. H. Zhang, Z. P. Zhuang, X. H. Wang, *J. Appl. Electrochem.* **2024**, *54*, 2193–2203.
[77] J. H. Li, Z. Q. Fan, H. P. Ye, J. Y. Zheng, J. W. Qiu, H. X. He, P. Liu, M. X. He, H. D. Liu, N. Y. Duchoa, R. H. Zeng, *Chem. Eng. J.* **2024**, *489*, 151188.
[78] G. H. Fang, Y. Pan, H. W. Yang, W. Chen, M. X. Wu, *J. Phys. Chem. C* **2024**, *128*, 6877–6886.

Manuscript received: July 12, 2024
Revised manuscript received: September 3, 2024
Accepted manuscript online: September 4, 2024
Version of record online: October 28, 2024